LIMNOLOGY
and
OCEANOGRAPHY: METHODS

ASLO

Limnol. Oceanogr.: Methods 17, 2019, 343–361

doi: 10.1002/lom3.10318

The dynamic ocean acidification manipulation experimental system: Separating carbonate variables and simulating natural variability in laboratory flow-through experiments

Iria Gimenez,[1,2,3]* **George G. Waldbusser**,[1] **Chris J. Langdon**,[4] **Burke R. Hales**[1]

[1]College of Earth, Ocean and Atmospheric Sciences, Oregon State University, Corvallis, Oregon
[2]Hakai Institute, Heriot Bay, British Columbia, Canada
[3]Department of Zoology, The University of British Columbia, Vancouver, British Columbia, Canada
[4]Coastal Oregon Marine Experimental Station, Department of Fisheries and Wildlife, Hatfield Marine Science Center, Oregon State University, Newport, Oregon

Abstract

Carbonate chemistry variables such as PCO_2, pH, and mineral saturation state (Ω) are commonly thought of as covarying in open-ocean settings but have decoupled over geologic time-scales and among modern dynamic coastal margins and estuaries. Predicting responses of vulnerable coastal organisms to past, present, and future ocean acidification (OA) scenarios requires the empirical identification of organismal sensitivity thresholds to individual carbonate chemistry parameters. Conversely, most OA experiments involve chemistry manipulations that result in covariance of carbonate system variables. We developed the Dynamic Ocean Acidification Manipulation Experimental System (DOAMES)—a feed-forward, flow-through carbonate chemistry control system capable of decoupling PCO_2, pH, or Ω by independently manipulating total alkalinity (TAlk) and total inorganic carbon (TCO_2). DOAMES proof-of-concept can manipulate source seawater with stable or variable carbonate chemistry and produce experimental treatments with constant and dynamic carbonate chemistry regimes. The combination of dynamic input and output allows for offset treatments that impose a ΔPCO_2 on naturally variable conditions. After overcoming several operational challenges, DOAMES is capable of simultaneously generating three different experimental treatments within 1% ± 1% of TCO_2 and TAlk targets. The achieved precision and accuracy resulted in the successful decoupling of pH and Ω_{Ar} in five trials. We tested the viability of sensitive bivalve embryos raised in DOAMES-manipulated seawater and found no difference in development when compared to the control, demonstrating DOAMES suitability for organismal studies. DOAMES provides a novel tool to evaluate organismal effects of exposure to decoupled carbonate system variables and to past, current, and future carbonate chemistry scenarios.

The uptake of atmospheric anthropogenic CO_2 by ocean surface waters has caused ocean acidification (OA) (Caldeira and Wickett 2003; Doney et al. 2009), a collective shift in marine carbonate chemistry that results in increased PCO_2 and reduced pH and calcium carbonate saturation state (Ω; Feely 2004; Honisch et al. 2012). OA is the consequence of the rapid increase in PCO_2 that cannot be compensated for by weathering of continental rocks or dissolution of marine carbonates (Honisch et al. 2012; Zeebe 2012). In contrast, geologic periods when the CO_2 release to the atmosphere was significantly slower than today such as the Miocene, Oligocene, and Cretaceous were associated with long-term decoupling of PCO_2, pH, and Ω due to the ability of Earth's system to partially buffer the rise in CO_2 (Honisch et al. 2012; Zeebe 2012).

Instances of decoupling do occur in the modern ocean over daily and monthly time-scales and result from the interaction of multiple physical and biological processes that alter carbonate chemistry (Fassbender et al. 2016). Decoupling, however, is more common on dynamic margins and coastal systems. For instance, in open ocean oligotrophic regions, where salinity, and thus alkalinity, do not vary significantly, temperature, net community production, air–sea gas exchange, and mixing dominate daily and seasonal changes in PCO_2 (Archer et al. 1996; Bates et al. 1998; DeGrandpre et al. 2004; Shadwick et al. 2015). Consequently, PCO_2 is generally tightly negatively correlated to pH and Ω, whereas pH and Ω are generally positively correlated to each other (Dore et al. 2009; Bates et al. 2012, 2014), although moderate seasonal and intraregional decoupling occurs due to differential thermal and salinity sensitivities (Takahashi et al. 2014).

*Correspondence: iria.gimenez@hakai.org

Iria Giminez's affiliation during this project was Oregon State University; her current affiliations are Hakai Institute and University of British Columbia.

Conversely, in dynamic coastal environments and estuaries, temperature and salinity vary significantly across daily and seasonal time-scales, and numerous physical and biological processes affect carbonate chemistry, including freshwater inputs, tides and regional circulation, seasonal upwelling, diel cycles of photosynthesis and respiration, and calcification and dissolution (Waldbusser et al. 2011; Fassbender et al. 2016; Hales et al. 2017; Pacella et al. 2018), all of which alter total inorganic carbon (TCO_2) and total alkalinity (TAlk) to different extents. As a result, instances of decoupling of PCO_2, pH, and Ω occur in daily, fortnightly, and seasonal time-scales (Cai et al. 2011; Waldbusser and Salisbury 2014; Evans et al. 2015; Hales et al. 2017).

Decoupling in coastal zones will also likely be exacerbated in the future, as modeled projections forecast increased high-frequency carbonate chemistry variability and different rates of change for PCO_2, pH, and Ω_{Ar}. For instance, Pacella et al. (2018) found that increased PCO_2 due to anthropogenic activity lowers buffering capacity in a seagrass habitat, therefore amplifying the effect of diel community metabolic cycles. The increased amplitude in TCO_2 changed daily maximum PCO_2 and minimum pH and Ω_{Ar} values more than 1.5X faster than the change in their median values. Changes in the seasonal variability of these carbonate parameters are also predicted and observed in open-ocean environments where decoupling is not prevalent (Kwiatkowski and Orr 2018; Landschützer et al. 2018). It follows, therefore, that to better predict future responses to OA of marine coastal organisms, current and future variability in carbonate chemistry parameters need to be incoporated in laboratory studies.

Resolving sensitivity mechanisms to different carbonate variables is more relevant in coastal organisms with identified heightened vulnerability to OA such as corals and bivalves (Kroeker et al. 2013). From an evolutionary perspective, many of the extant taxa of bivalves, for instance, evolved during the Triassic and Cretaceous periods, with extensive evolutionary radiation occurring during the latter (Crame 2000). Both of these geological periods coincided with likely episodes of natural decoupling of pH and Ω_{Ar} (Kump et al. 2009; Honisch et al. 2012; Zeebe 2012); therefore, observed bivalve differential sensitivities to carbonate chemistry parameters such as PCO_2, pH, and Ω_{Ar} in present conditions (Waldbusser et al. 2015*a*, *b*; Thomsen et al. 2015*b*; Waldbusser et al. 2016*b*) might stem from evolutionary adaptations. The differential decoupling of carbonate system variables today vs. in the geologic past and the complex carbonate chemistry dynamics in coastal and estuarine systems have broad implications for understanding species responses to OA in an evolutionary context, as well as how we design experiments to better predict future changes in marine communities.

Most OA experiments to date rely on injection or bubbling of CO_2 gas as the mechanism to generate carbonate chemistry treatments (see reviews by Kroeker et al. [2010] and Cornwall and Hurd [2015]). CO_2 bubbling, albeit it can recreate changes in the carbonate system associated with photosynthesis or respiration, typically generates tightly controlled experimental conditions that also closely mimic changes in marine carbonate systems associated with the very rapid anthropogenic perturbation of atmospheric CO_2. Thus, this approach was codified after the publication of the "Guide to best practices for OA research and data reporting" guidelines (Gattuso et al. 2010). Experiments based on CO_2 bubbling, therefore, have been crucial in documenting the adverse physiological effects associated with OA across multiple taxa and life-stages (reviewed in Kroeker et al. [2010, 2013] and Wittmann and Pörtner [2013]). While mimicking the current global changes in marine carbonate chemistry, this manipulation technique, however, results in the covariance of PCO_2, pH, and Ω, and thus leads to equivocal experimental interpretations as the true driver of response is difficult to isolate empirically. Similarly, field observations across naturally covarying acidification gradients (e.g., Cigliano et al. 2010; Kroeker et al. 2011) provide valuable insight but often lack the power to discriminate physiological mechanisms underlying responses (i.e., Waldbusser et al. 2015*a*, *b*). Thus, the interpretation of physiological responses to OA is confounded, due to the inability to attribute which variable is causing the observed effects, therefore precluding a mechanistic understanding of the drivers of organismal sensitivity. Hence, carbonate chemistry manipulation techniques that empirically decouple PCO_2, pH, and Ω are essential.

Short-term physiological responses to different carbonate system variables have been explored by the development of batch-culture manipulation laboratory techniques specifically designed to decouple carbonate chemistry parameters. Although temperature and salinity are often the ultimate multidrivers of carbonate chemistry decoupling in coastal zones, most manipulation techniques keep these environmental variables stable and rely on direct changes to the carbonate chemistry system itself to decouple PCO_2, pH, and Ω and assess organismal sensitivity. For instance, decoupling techniques based on altering TCO_2 and/or TAlk have been used to study biocalcification in corals, bivalve larvae, and coccolithophores (Schneider and Erez 2006; Jury et al. 2010; Gazeau et al. 2011; Bach et al. 2013; Thomsen et al. 2015*a*; Waldbusser et al. 2015*a*, *b*; Comeau et al. 2017). In these experiments, biocalcification was largely insensitive to pH and PCO_2, but controlled by Ω_{Ar} (Waldbusser et al. 2015*a*, *b*), $[CO_3^{2-}]$ (Gazeau et al. 2011), or $[HCO_3^-/H^+]$ (Bach et al. 2013; Jokiel 2013; Thomsen et al. 2015*a*), although combinations of multiple variables have also been invoked (e.g., Bach et al. 2013; Comeau et al. 2017). Conversely, respiration on early-larval mussels is negatively impacted by low pH (Waldbusser et al. 2015*b*), while feeding responses in early bivalve larvae appear to be driven by PCO_2 or Ω_{Ar} (Waldbusser et al. 2015*b*; Gray et al. 2017). The diversity of carbonate chemistry drivers of short-term physiological responses warrants further exploration to elucidate modes of action of long-term exposure to acidified conditions and, ultimately, mechanisms of sensitivity to improve our predictions of OA long-term effects in organisms.

Long-term exposure experiments, crucial to investigate multigenerational and chronic or sublethal physiological effects of OA, require different experimental approaches. While

batch-culture experimental techniques have provided very valuable insight, they are less suitable for long-term exposure experiments, can result in "bottle effects" on carbonate chemistry and limit approaches designed to assess organismal responses to dynamic chemistry conditions (e.g., Frieder et al. 2014; Clark and Gobler 2016). Long-term exposure experiments that utilize destructive sampling generally require higher density of organisms and, therefore, benefit from flow-through culture systems that prevent targeted carbonate chemistry conditions from deviations resulting from in situ respiration and photosynthesis (e.g., Rost et al. 2008; Gradoville et al. 2014) and reduce the accumulation of metabolic waste products. Furthermore, flow-through experimental designs allow for the simulation of variable carbonate chemistry conditions often experienced by organisms in the coastal environment, a research priority identified by the OA community (Takeshita et al. 2015; Boyd et al. 2016; Wahl et al. 2016).

In order to adress the need from experimental systems that both decouple carbonate chemistry variables through the alteration of TAlk and TCO_2 and provide flow-through conditions with long term, controlled carbonate chemistry treatments, we: (1) adapted the short-term, batch-culture techniques developed in Waldbusser et al. (2015*a*, *b*)) and Waldbusser et al. (2016*b*) (*see* also Schneider and Erez 2006; Jury et al. 2010; Keul et al. 2013), for the development of the dynamic ocean acidification manipulation experimental system (DOAMES)—a feed-forward, flow-through carbonate chemistry control system capable of long-term, automatic decoupling of carbonate chemistry parameters (i.e., pH and Ω_{Ar}) by performing precise manipulations of TAlk and TCO_2; (2) evaluated DOAMES performance with variable and stable source seawater inputs and with dynamic and offset carbonate chemistry targets; and (3) performed a proof-of-concept validation of DOAMES by exposing sensitive early stages of bivalve larvae to highly acidified seawater that DOAMES returned to favorable carbonate conditions for larval development.

Materials and procedures

Experimental system overview

DOAMES independently and automatically manipulates TAlk and TCO_2, the master variables of the carbonate system, in two stages: (1) real-time measurement of source seawater PCO_2 and TCO_2 through a continuous nondispersive infrared (NDIR)-based analyzer and computation of all carbonate chemistry variables and (2) a feed-forward control system to achieve user-defined targets of TAlk and TCO_2 via high-precision mineral acid–base additions to the source seawater (Fig. 1).

Description of DOAMES hardware: NDIR-based continuous PCO_2 and TCO_2 analyzer

The PCO_2 and TCO_2 analyzer measures inlet water chemistry by temporally alternating the analysis of PCO_2 and TCO_2 and is based on published designs of high-frequency, continuous PCO_2 and TCO_2 systems (Hales et al. 2004; Bandstra et al. 2006; Vance 2012). In this application (described further below), it

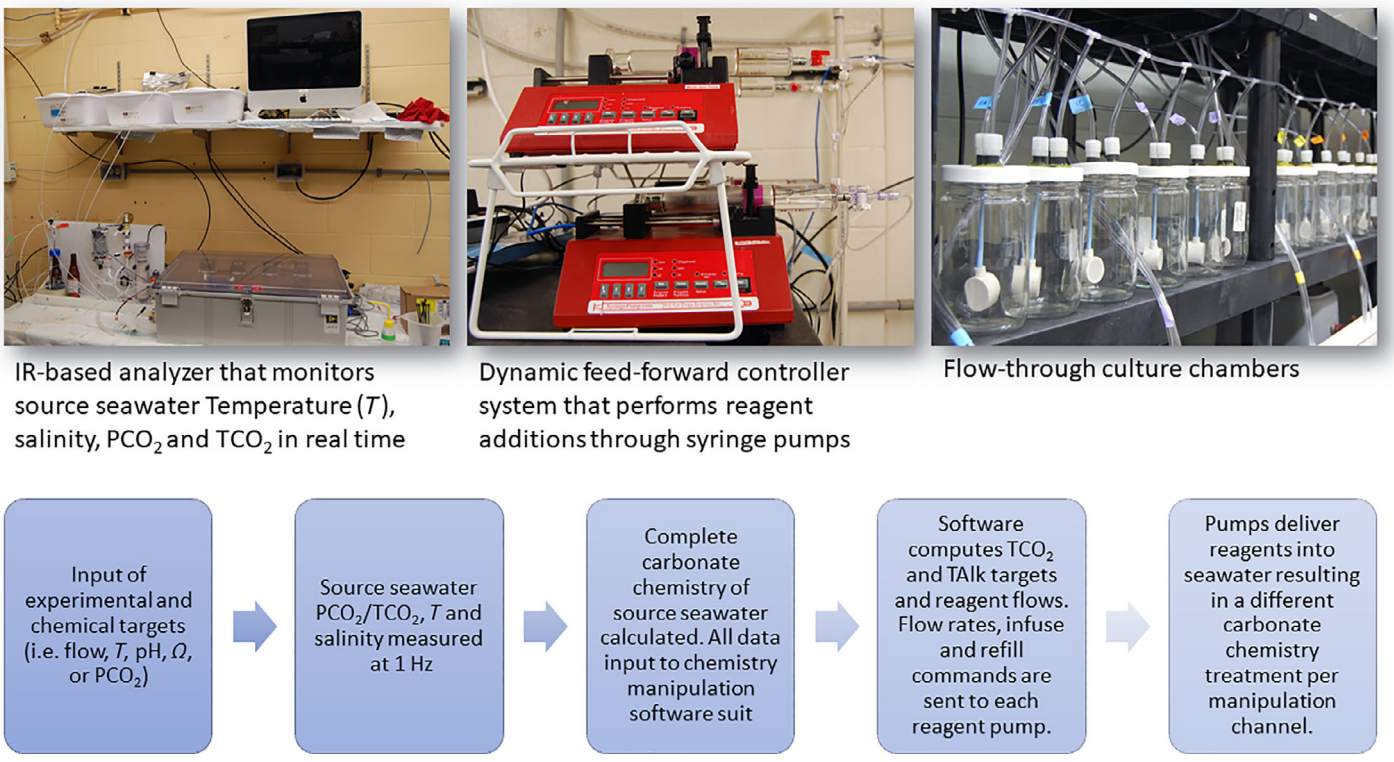

Fig. 1. Step-by-step description of the DOAMES manipulation protocol and components.

was necessary to recirculate water between the holding tank and the experimental apparatus, and so a microporous hydrophobic membrane contactor (3M Liqui-Cel EXF-2.5x8 Series Membrane Contactor, Liqui-Cel) was used for PCO_2 equilibration (following Hales et al., 2004; Bandstra et al., 2006) rather than a gravity-draining showerhead-style equilibrator. Briefly, filtered sea water (1–10 μm, nominally) was routed through a thermosalinograph (SBE 45 MicroTSG, Sea-Bird Scientific) to measure salinity and temperature at a flow rate of 2–6 L min^{-1}. Flow subsequently entered the LiquiCel unit, where rapid gas transfer between the recirculated gas analytical stream and the water stream ensured efficient gas-phase equilibration of the gas stream with the water PCO_2. The equilibrated gas stream is then routed through an NDIR absorbance CO_2 detector (LI-840A, LI-COR) for analysis. In parallel with this flow regime, a split of sample water is drawn from the main sample flow (one to four times per hour for 3 min at a time) at a flow rate of 20 mL min^{-1} and acidified with 10% HCl to convert all carbonate and bicarbonate to $CO_{2,aq.}$ This aqueous CO_2 is then stripped from solution using a 900 mL min^{-1} flow of CO_2-free gas in a smaller membrane contactor (3M Liqui-Cel MM-1.0x5.5 Series Membrane Contactor, Liqui-Cel). The mass-balance-determined CO_2 content of this strip-gas stream is subsequently determined by the NDIR CO_2 detector. Temperature, salinity, and gas stream CO_2 content measurements were made at 1 Hz, and the response times of the PCO_2 and TCO_2 measurements are estimated at 5 and 15 s, respectively, as shown in Hales et al. (2004) and Bandstra et al. (2006).

Every 6 h, automatically, or at any user-defined interval, the NDIR detector is calibrated using two or more certified gas standards (CO_2 in Ultrapure Air, Scott-Marrin). Similarly, three or more liquid TCO_2 standards are also analyzed to calibrate the TCO_2 measurements across the expected measurement range. Finally, upon user-input, the analyzer can be used to measure PCO_2 and TCO_2 in discrete samples by temporarily pausing continuous measurements and utilizing the sample-equilibrator mode. In discrete mode, we measured PCO_2 by equilibrating the sample headspace gas and bypassing the membrane contactor and TCO_2 by analyzing the discrete sample instead of the seawater streamflow.

These measurements and calibrations are used to continuously and automatically calculate the remaining parameters of the carbonate system following water dissociation constants from (Millero 1995), carbonic acid equilibration constants from Millero (2010), Dickson (1990) constants for boric acid and calcite, and aragonite solubility constants from Mucci (1983). The DOAMES carbonate chemistry manipulation software (detailed below) then incorporates all the calculated data.

The PCO_2/TCO_2 software, based in LabVIEW (National Instruments, NI, version 2012), integrates communication and automatic control of all pumps, mass flow controllers, sensors, and data acquisition boards through a user-friendly control panel. Additionally, we designed the software to automatically log data and metadata, as well as process, compute, and visualize preliminary data. A version of this continuous PCO_2/TCO_2 analyzer is commercially available under the brand name Burke-O-Lator (Dakunalytics, LLC).

Description of DOAMES hardware: Feed-forward TCO_2 and TAlk manipulation system

The carbonate chemistry manipulation component of DOAMES coordinates the delivery of seawater and reagents necessary to produce the desired experimental treatments. We developed DOAMES to produce three independent experimental treatments, albeit it can be easily expanded to accommodate additional treatments. Following DOAMES experimental system diagram (Fig. 2, blue box), source seawater is routed from the outlet of the membrane contactor through in-line heaters (Heater for External Canister Filters, Hydor) and heated to the targeted experimental temperature. Subsequently, one metering, positive displacement pump (FMI QV, Fluid Metering Inc.) coupled with a variable flow pump head (RH1, Fluid Metering Inc.) delivers heated seawater for each manipulation channel (i.e., experimental treatment). A variable speed controller (V300, Fluid Metering Inc.), set via an analog voltage signal, drives the pump. We gravimetrically calibrated each combination of controller and pumps to obtain a voltage–flow linear relationship. The minimum and maximum flows tested were 73 and 113 mL min^{-1} for each treatment, which corresponded to 50% and 70% of the maximum voltage signal, respectively.

Each manipulation channel consists of two pairs of variable flow, programmable syringe pumps (NE-100, New Era Pump Systems Inc.): (1) one pair delivers the mineral acid reagent: 0.1 mol L^{-1} HCl, gravimetrically diluted from certified 1.0 mol L^{-1} HCl (5620–07, J.T. Baker, or BDH7202-7, BDH VWR Chemicals), and (2) one pair delivers the mineral base reagent: a concentrated solution of reagent-grade Na_2CO_3 (7527-06, Macron Fine Chemicals) and $NaHCO_3$ (7412-06, Macron Fine Chemicals) in deionized water with the Na_2CO_3 : $NaHCO_3$ ratio targeted to produce approximately ambient atmospheric PCO_2 values so that the effects of gas exchange were minimized during preparation and transfer to gas-impermeable bottles. All syringe pumps are fitted with gravimetrically calibrated 60 mL luer-lock polypropylene syringes (309653, BD Medical) to ensure volumetric dispensing accuracy.

Each pair of reagent pumps connects to a four-port, two-position switch valve (C22, Valco Instruments Company Inc.). One port is plumbed to the reagent reservoir, two ports are linked to each of the paired syringes, and the fourth port connects to the reagent outflow. The valve's position determines two flow paths: (1) reservoir to the filling syringe and (2) injecting syringe to outflow (Fig. 3). An electric actuator controls the switch between flow paths, interfacing with the manipulation software to synchronize refilling-injection routines and ensure constant delivery of reagent.

Both reagent outflows are combined in a mixing coil prior to their injection into each manipulation channel to avoid mineral precipitation observed in earlier versions, a result of the direct addition of a strong base to seawater. The injection point is located immediately downstream from the seawater metering pumps and consists of an in-line T-fitting with an associated one-way polypropylene or styrene–acrylonitrile check-valve (PP695-2B2BF HAST, Pneuline Supply Inc.; or EW-30505-92, Cole-Parmer) to prevent seawater back-flow.

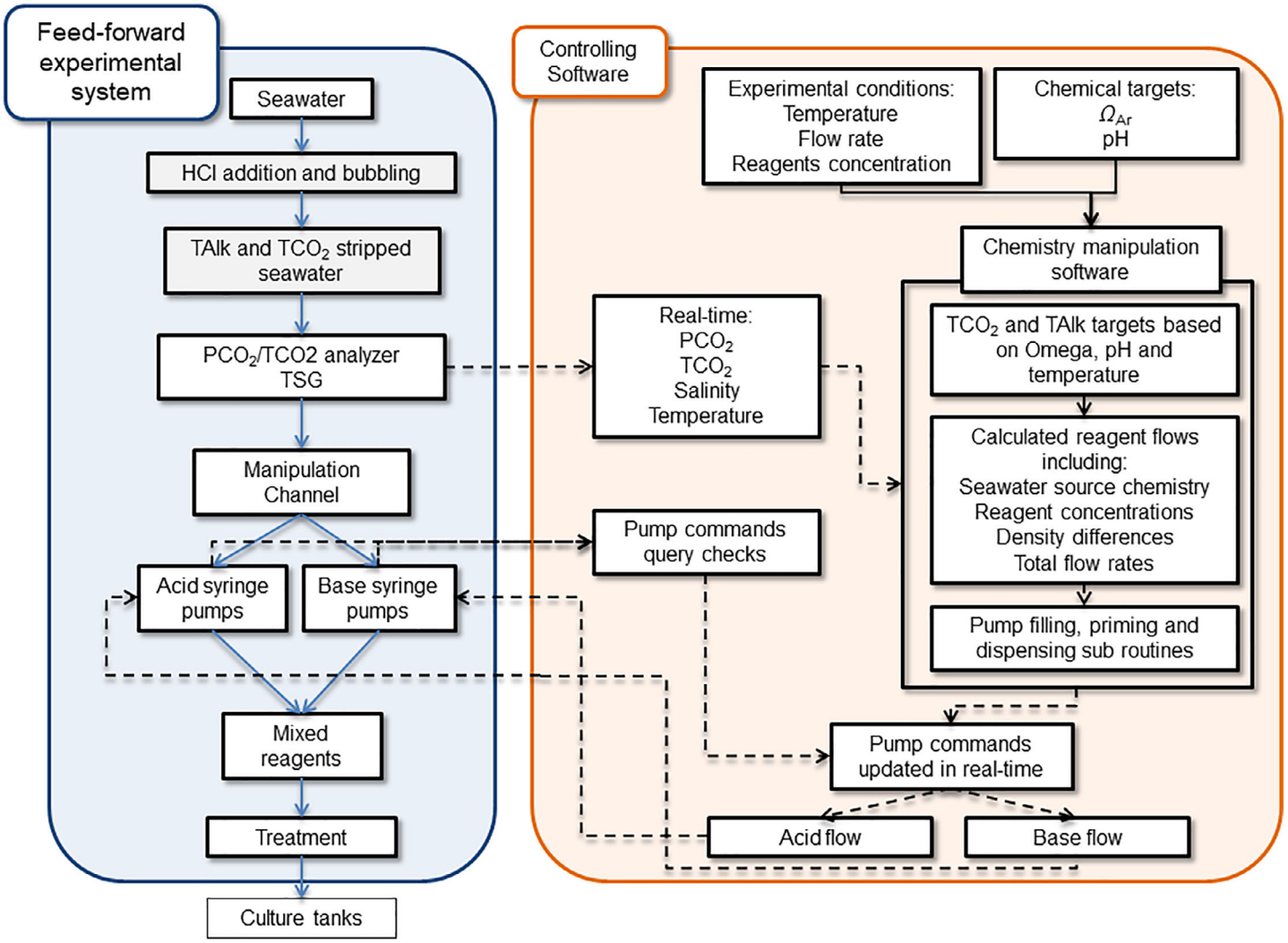

Fig. 2. DOAMES conceptual diagram. In blue, the hardware components of the experimental system. In orange, the controller software architecture. Shaded boxes (e.g., "HCl addition and bubbling" and "TAlk and TCO_2 stripped water") show stages of the experimental system that are only included in some manipulation experimental designs. Solid, blue arrows represent the flow of seawater and manipulation reagents. Solid, black arrows represent static inputs of information set by the user. Dashed, black arrows represent dynamic inputs of information updated in real time (<1 min). Feed-backs within and across both components of the system are shown by dashed arrows crossing boxes.

Description of DOAMES: Manipulation software

DOAMES' controlling software integrates the calculation of target reagent flows based on source seawater carbonate chemistry and the automatic control of DOAMES' hardware components (Fig. 2, orange box). A stand-alone program developed using LabVIEW controls each manipulation channel, thereby providing a level of architectural redundancy that prevents the stop of all manipulation channels in the event of a single pump communication failure. Before initialization of the program, the user manually sets the experimental targets for both TAlk and TCO_2 (based on desired targets of Ω, pH, and/or PCO_2), the flow rate of the seawater-delivery pump for each manipulation channel, base reagent (TAlk and TCO_2), and acid reagent concentrations, and the target temperature for the experimental treatments. All of these experimental parameters are entered in the front screen of the controlling software (Fig. 4) and can be modified at any time. Although DOAMES does not control any of these experimental parameters, they are incorporated in the calculations to determine reagent flow rates.

Upon initialization, the software reads real-time–processed data from the TCO_2/PCO_2 analyzer at a frequency of 1 Hz and updates source–seawater measurements of temperature, salinity, PCO_2, TCO_2, and calculated TAlk values. These data, along with the experimental parameters defined by the user discussed above, are then used to compute reagent flow rates automatically. Flow rates of reagents depend on the desired targets of TAlk and TCO_2 and the initial carbonate chemistry values of the source seawater but generally range between 1% and 5% of the total seawater flow rates.

A subroutine then communicates with each pair of syringe pumps, updates the injecting flow rates and the volume

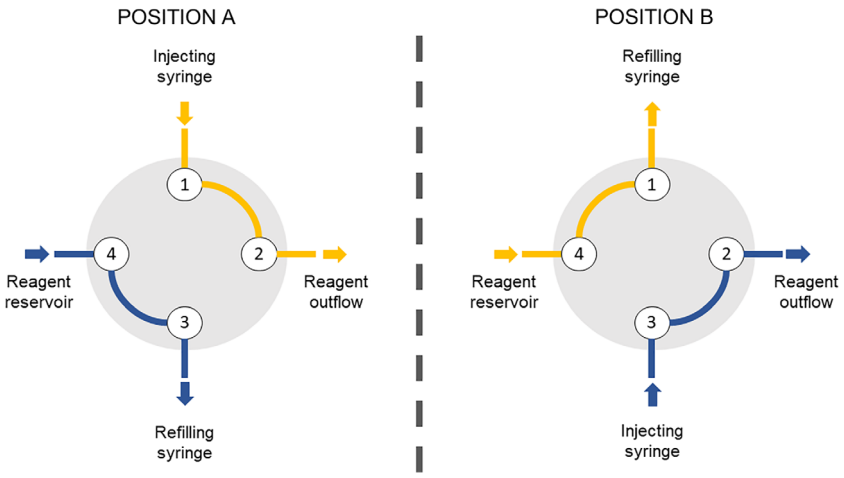

Fig. 3. Schematic diagram of the two available positions of each reagent switch valve.

dispensed by injecting syringes, determines the refilling flow rate on the refilling syringes, and controls switching of both reagent valves. Additionally, the software automatically performs data logging of all relevant input and calculated data.

Laboratory tests

We evaluated the performance of DOAMES in eight trials conducted between 2015 and 2017 at the Hatfield Marine Science Center (HMSC), Newport, Oregon (Table 1). In these trials, we assessed DOAMES capability to decouple pH and Ω_{Ar}, as well as to manipulate a dynamic source of seawater and simultaneously produce stable, dynamic, and offset experimental treatments.

Modes of carbonate chemistry manipulation experiments

Decoupling of pH and Ω_{Ar}

We performed seven trials between 2015 and 2017 to experimentally decouple pH and Ω_{Ar} due to the recent interest in this topic (Cyronak et al. 2016; Fassbender et al. 2016; Waldbusser

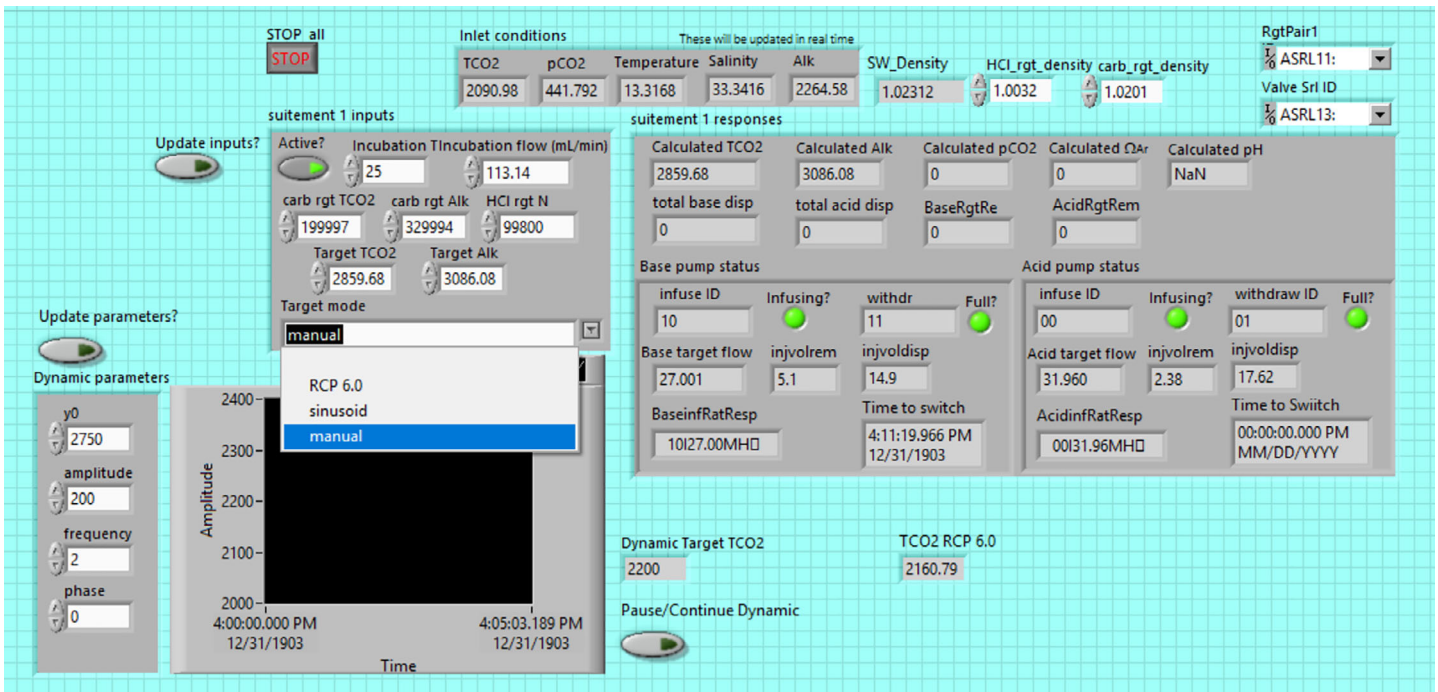

Fig. 4. DOAMES software control panel. The main screen includes the source seawater (inlet) conditions (top center) and the user-defined manipulation parameters including temperature, flow, reagent concentrations, and TAlk and TCO_2 targets (center). The input tab box also includes the target mode drop-down menu, with the options of manual, dynamic (sinusoid), or RCP 6.0 targets (*see* text). User-defined parameters for the dynamic manipulation mode, as well as a graphical time-series and instantaneous values of dynamic and RCP6.0 targets are shown at the bottom. The calculated TCO_2 and TAlk values as well as the status and calculated target flow rates of reagent pumps are shown in the responses tab (center right).

Table 1. DOAMES accuracy and precision across trials. The 2017 trials were excluded from the overall accuracy and precision due to mechanical fatigue of reagent pumps (*see* Discussion section). Best DOAMES performance was achieved on March 2016.

Date	Source seawater	Type of manipulation targets	TCO_2 % absolute relative error*	TAlk % absolute relative error*
April 2015	Stable	Mimic control conditions	2.3 ± 2.7	3.8 ± 5.1
October 2015	Stable	Constant Ω_{Ar} and varying pH	2.0 ± 2.8	3.2 ± 3.8
March 2016	Stable	Constant Ω_{Ar} and varying pH	1.2 ± 0.9	1.2 ± 0.9
April 2016	Stable	Constant Ω_{Ar} and varying pH	4.1 ± 1.3	4.6 ± 1.4
June 2016	Dynamic	Stable, dynamic and offset	1.5 ± 1.5	2.3 ± 1.9
July 2016	Stable	Constant Ω_{Ar} and varying pH	4.9 ± 2.9	4.5 ± 2.5
August 2016	Stable	Constant Ω_{Ar} and varying pH	4.8 ± 2.6	4.9 ± 3.1
February 2017	Stable	Constant Ω_{Ar} and varying pH	5.1 ± 3.0	5.0 ± 4.1
March 2017	Stable	Constant Ω_{Ar} and varying pH	3.6 ± 4.8	5.1 ± 7.0
Overall†			2.1 ± 2.4	2.9 ± 3.1
Best performance			1.2 ± 0.9	1.2 ± 0.9

* ± are standard deviations.
†Excluding 2017 trials (*see* Assessment section).

et al. 2016*a*). We first developed the manipulation software to accept user inputs of TAlk and TCO_2 targets that remained stable during the test (Fig. 4; manual). We designed DOAMES three simultaneous manipulation treatments to cover a constant Ω_{Ar} across a range of three pH values (from 7.55 to 7.85), one for each manipulation channel. We conducted these experiments at two different temperatures (20°C and 25°C) and, therefore, target Ω_{Ar} values varied between 2.00 and 3.00 (Table 2).

We carried the decoupling experiments with stable source seawater by partially filling 1500 liters reservoir tanks with an approximate volume of 1250 liter of filtered seawater. The seawater at the laboratory tended to have significantly supersaturated PCO_2 and so was vigorously aerated with outdoor ambient air for a minimum of 8 h to stabilize its PCO_2 value before carbonate chemistry manipulations. There are seawater targets that require removing TCO_2 to reach target values (e.g., low Ω_{Ar}), and for these, seawater may need to be stripped of TCO_2 and TAlk before manipulations. For this reason, in some trials, source seawater's TAlk was partially titrated through the addition of reagent-grade, concentrated HCl, and subsequently TCO_2 was stripped by vigorous aeration. It is important to note that the bubbling is not a critical step in the procedure, as the true TCO_2 and PCO_2 values were measured continuously before the manipulation reagents were added. Similarly, although prolonged heavy bubbling under very dry atmospheres can lead to increased salinity, salinity is constantly monitored by the PCO_2/TCO_2 analyzer and significant changes can thus be detected and corrected.

The seawater was continuously recirculated from the holding tank to the PCO_2/TCO_2 analyzer, except for the necessary flow of water needed for treatments (a maximum of ~350 mL min^{-1}). In these trials, designed to mimic the optimal conditions to run Pacific oyster larvae experiments (Waldbusser et al. 2015*a*), the temperature of the recirculating source seawater was kept below 15°C to minimize pathogenic bacterial growth (*Vibrio* spp.) by use

Table 2. Ω_{Ar} and pH_t decoupling experiments' mean experimental results.

			Manipulation channel 1*		Manipulation channel 2*		Manipulation channel 3*	
Date	Temperature* (°C)	Salinity*	Target	Observed	Target	Observed	Target	Observed
October 2015	20.1 ± 0.5	32.7 ± 0.0	Ω_{Ar} = 2.50; pH_t = 7.85	Ω_{Ar} = 2.19 ± 0.57; pH_t = 7.79 ± 0.13	Ω_{Ar} = 2.50; pH_t = 7.70	Ω_{Ar} = 3.03 ± 1.66; pH_t = 7.77 ± 0.18	Ω_{Ar} = 2.50; pH_t = 7.50	Ω_{Ar} = 2.17 ± 0.66; pH_t = 7.50 ± 0.13
March 2016	20.2 ± 0.2	28.6 ± 0.0	Ω_{Ar} = 2.52; pH_t = 7.89	Ω_{Ar} = 2.50 ± 0.27; pH_t = 7.89 ± 0.05	Ω_{Ar} = 2.50; pH_t = 7.74	Ω_{Ar} = 2.61 ± 0.24; pH_t = 7.75 ± 0.04	Ω_{Ar} = 2.47; pH_t = 7.58	Ω_{Ar} = 2.77 ± 0.38; pH_t = 7.63 ± 0.06
April 2016	19.4 ± 0.3	31.8 ± 0.0	Ω_{Ar} = 2.52; pH_t = 7.89	Ω_{Ar} = 2.46 ± 0.04; pH_t = 7.85 ± 0.02	Ω_{Ar} = 2.50; pH_t = 7.74	Ω_{Ar} = 2.87 ± 0.60; pH_t = 7.77 ± 0.09	Ω_{Ar} = 2.47; pH_t = 7.58	Ω_{Ar} = 2.85 ± 0.48; pH_t = 7.62 ± 0.07
July 2016	25.1 ± 0.4	33.2 ± 0.3	Ω_{Ar} = 3.00; pH_t = 7.85	Ω_{Ar} = 2.89 ± 0.20; pH_t = 7.84 ± 0.03	Ω_{Ar} = 3.00; pH_t = 7.70	Ω_{Ar} = 3.18 ± 0.54; pH_t = 7.74 ± 0.07	Ω_{Ar} = 3.00; pH_t = 7.55	Ω_{Ar} = 3.38 ± 0.80; pH_t = 7.62 ± 0.10
August 2016	25.1 ± 0.2	33.7 ± 0.0	Ω_{Ar} = 3.00; pH_t = 7.85	Ω_{Ar} = 2.59 ± 0.64; pH_t = 7.78 ± 0.13	Ω_{Ar} = 3.00; pH_t = 7.70	Ω_{Ar} = 2.95 ± 0.47; pH_t = 7.70 ± 0.07	Ω_{Ar} = 3.00; pH_t = 7.55	Ω_{Ar} = 3.00 ± 0.39; pH_t = 7.57 ± 0.06

* ± are standard deviations.

of a seawater chiller (C-0500, Resun). The manipulated seawater was, therefore, heated inline to match the target temperature before delivery to experimental containers.

Dynamic source seawater

In some instances, performing experimental studies without reservoir tanks and directly from a seawater feed-line might be advantageous. For instance, if there are concerns regarding water quality deterioration over time due to stagnation, if there is interest in replicating natural carbonate chemistry variability, or if the capability to hold salinity or temperature constant is compromised. As a consequence, we tested DOAMES performance in a reservoir-less manipulation trial conducted in June 2016 to assess the capability of the system to reliably produce manipulated treatments with dynamic sources of seawater. To that end, we performed this experiment by directly analyzing and manipulating the laboratory incoming seawater continuous streamflow.

Stable, dynamic, and offset targets

We ran a 1-week-long trial using the dynamic live seawater system from the HMSC in June 2016 (Table 1). In this trial, we produced three simultaneous different carbonate chemistry treatments: a stable set of targets, a combination of idealized dynamic TCO_2 and stable TAlk, and an offset from the naturally variable water coming into the system.

In the stable manipulation channel, the TCO_2 and TAlk targets were manually set (Fig. 4; manual) to 2750 and 2980 μmol kg^{-1}, respectively, throughout the entire trial.

In the second manipulation channel, we modified the software to allow for user input of mean, amplitude, and frequency of the sinusoid signal (Fig. 4; sinusoid). We then tested this capability by defining an idealized sinusoid pattern for TCO_2 that mimic a semidiurnal signal centered around a value of 2750 μmol kg^{-1} with a mean amplitude of 200 μmol kg^{-1} (2750 $\pm$ 200 μmol kg^{-1}) and a frequency of 2 cycles d^{-1}. Simultaneously, we kept the TAlk target constant (3000 μmol kg^{1} for the first 6 d; 2900–2950 μmol kg^{-1} for the last day of the experiment).

The TCO_2 and TAlk targets for both the first and second manipulation channels fell outside the usual range found in marine environments. These values, however, were chosen as a rigorous test for DOAMES dynamic capabilities, as they imposed demanding reagent delivery requirements.

In the third manipulation channel, we created a set of constant offset conditions meant to preserve the naturally dynamic carbonate chemistry from a given location and add a constant amount of anthropogenic carbon to those variable conditions (Fig. 4; Representative Concentration Pathways [RCP 6.0]). This type of carbonate chemistry manipulation test calculated the TCO_2 target based on an offset ΔPCO_2 imposed on the continuous source seawater PCO_2 values. We estimated ΔPCO_2 as the difference between current, global atmospheric CO_2 and the 2100 atmospheric CO_2 predicted from future Intergovernmental Panel on Climate Change (IPCC) projections according to different RCPs (e.g., RCP 6.0; Pachauri et al. 2015; Fig. 4). We designed the software logic to continually compute the instantaneous source seawater PCO_2 by adding ΔPCO_2 to the measured PCO_2 value. Subsequently, DOAMES computed the resulting TCO_2 value with the corrected source seawater PCO_2, together with the original TAlk, temperature, and salinity values. The software then updated the resulting TCO_2 value as the manipulation target value. We allowed the TAlk target to dynamically vary mimicking the naturally variable alkalinity value of the source seawater.

Organismal exposure to manipulated carbonate chemistry test

In April 2015, we tested DOAMES applicability to organismal acidification stress experiments by exposing early stages of Pacific Oyster (*Crassostrea gigas*) larvae to manipulated seawater from fertilization to 48 h postfertilization. We utilized static culture chambers as controls to help separate any potential effects of flow from the carbonate chemistry manipulations on larval development. In previous work, we have demonstrated the ability to culture oyster larvae with high fidelity, resulting in upward of 80% embryo development (Waldbusser et al. 2015*a*). Therefore, we had to ensure that DOAMES did not have a significant effect on the development of larvae.

To do this, we acidified and stripped the source seawater to reduce the TCO_2 and TAlk, and then manipulated the carbonate chemistry to return to the control, unaltered conditions of the source seawater. Initially, both the unaltered and manipulated flow-through reservoir tanks were filled with filtered seawater heavily aerated with outside, ambient air. The DOAMES reservoir tank was then acidified and purged with ambient air to reduce the TAlk and TCO_2 by ~80%. In this experiment, we used only one manipulation channel, and targets for both TAlk and TCO_2 were set to 2145 and 1958 μmol kg^{-1}, respectively, matching the carbonate chemistry values of the control seawater measured at the start of the experiment. Embryos were then raised in both control and manipulated water, in both static and flow-through conditions. As a negative control, embryos were also reared in static, acidified, unmanipulated source seawater from the DOAMES reservoir tank.

Spawn and larval culture

Spawning, fertilization, and embryo viability assessments were conducted following previous protocols (Waldbusser et al. 2015*a*, *b*). Briefly, we obtained multiple male and female Pacific oyster broodstock from Whiskey Creek Shellfish Hatchery and manually stripped them of their gametes on 07 April 2015. The gametes were subsequently pooled and fertilized in filtered seawater. After 2 h postfertilization, we checked fertilization success by assessing the appearance of polar bodies. Developing embryos were then transferred to 500 mL biological oxygen demand (BOD) bottles or 1 liter borosilicate glass culture chambers (1397-1L, Corning), for static or flow-through culture, respectively. The embryos were cultured in five replicate culture chambers per treatment and at stocking densities of 10 embryos mL^{-1} for static and 25 embryos mL^{-1} for flow-through cultures. Each flow-through

culture chamber inlet was connected to DOAMES manipulation channel outflow, whereas the outlets of all treatment chambers were plumbed to a multichannel peristaltic pump (Masterflex) that regulated an equal inflow of manipulated water at a constant flow rate of 1 mL min^{-1} across all treatment replicate culture chambers. Each chamber was sealed to maintain a constant headspace of approximately 100 mL and to ensure that the inflow and outflow rates would be equal, thus simplifying the flow calibration procedure. The outlet was also fitted with a 20 μm "banjo-type" Nitex filter to allow for the flow of seawater but prevent the loss of organisms.

The experiment terminated approximately at 48 h postfertilization. Larvae from each BOD bottle and culture chamber were collected and preserved with 10% formalin diluted in deionized water and buffered to a pH of ~ 8.15. Discrete carbonate chemistry samples were obtained from each culture chamber upon termination of the experiment. We examined larvae under an inverted light microscope to evaluate the proportion of normally developed larvae with respect to the total number of larvae, following established criteria (His et al. 1997; Waldbusser et al. 2015*a*, *b*, 2016*b*).

Discrete carbonate chemistry samples

Discrete carbonate chemistry samples from experimental treatments were routinely obtained from the outflow of each manipulation channel at flows greater than 40 mL min^{-1} or from the outflow of culture chambers when flow rates were greater than 7 mL min^{-1}. Samples were collected in 350 mL amber glass bottles with polyurethane-lined crimp-sealed metal caps and immediately analyzed or preserved with 100 μL of saturated $HgCl_2$ solution for later analysis. In situ temperature and salinity values were recorded, and TCO_2 and PCO_2 were measured in the abovementioned PCO_2/TCO_2 analyzer by temporarily switching from continuous mode to discrete sample analysis. Alternatively, we analyzed preserved samples in an analogous PCO_2/TCO_2 system dedicated to discrete sample analysis. The estimated, combined analytical uncertainty is 0.2% for TCO_2 and 2% for PCO_2 (Hales et al. 2017), based on analysis of certified reference materials provided from A. Dickson's laboratory at the Scripps Institution of Oceanography. As detailed in the DOAMES description section, the remaining parameters of the carbonate system were calculated following water dissociation constants from Millero (1995), carbonic acid equilibration constants from Millero (2010), Dickson (1990) constants for boric acid and calcite, and aragonite solubility constants from Mucci (1983).

Data analysis

Carbonate chemistry manipulations

We assessed the overall performance of DOAMES, in terms of accuracy and precision of the carbonate chemistry manipulations, by evaluating the relative error as the difference between actual conditions and target values, divided by the target values. We report the absolute value of this error and assessed systematic errors in the sign-retaining error through one-sample Student's *t*-tests. We further evaluated the successful separation of pH treatments under constant Ω_{Ar} through one-way analysis of variance (ANOVA) with manipulation treatment as a factor.

Larval development

We square-root arcsine-transformed the larval development data and analyzed them through one-way ANOVA with treatment as a factor. All statistical analyses were performed in Rstudio (version 1.0.136).

Assessment

Overall accuracy and precision of carbonate chemistry manipulations

Although the overall accuracy and precision of the system, excluding 2017 trials, is 2.1% ± 2.4% for TCO_2 and 2.9% ± 3.1% for TAlk (Table 1), DOAMES is capable of 1.2% and a precision of ±0.9% for both TCO_2 and TAlk when mechanical and software operation challenges are minimized, thereby a more representative assessment of DOAMES' capabilities (Table 1).

Initial target achievement was 2.3% and 3.8% for TCO_2 and TAlk, respectively, with an associated precision of 2.7% for TCO_2 and 5.1% for TAlk. After we identified several operational problems, including mechanical and software inadequacies, we implemented system modifications including enhancements of syringe pumps' mechanical stability, redesign of the reagent injection system, including check-valves and switching valves, and improvements of the communication between syringe pumps and controlling software. As we overcame these challenges, manipulation's accuracy improved by two-fold (TCO_2) to three-fold (TAlk), whereas precision improved three- to six-fold for TCO_2 and TAlk, respectively, when comparing stable manipulations between April 2015 and March 2016 (Table 1; Fig. 5).

We chose syringe pumps because the linear-actuation mechanism coupled with a high-resolution stepper-motor controller in theory provides the greatest dynamic range of positive-displacement flow control; however, syringe pumps in general, and NE-100 pumps in particular, provided several operational challenges. First, syringe pumps required a pair of pumps for each reagent and complicated logic to monitor flow volume and control rates through switching procedures. Across all trials, a pattern emerged of periodic outliers of discrete sample values with % relative error greater than 7% for either (or both) manipulated variables, sometimes associated with overlapping switching routines for both reagent pumps, resulting in transient instances (<30 s) of completely paused manipulations. We hypothesize that the overall effect of these transient reagent delivery failures on experimental treatments will mostly depend on the frequency of occurrence, the residence time of the culture chambers, and the difference in carbonate chemistry conditions between the source seawater and the experimental treatment. Second, the NE-100 pumps had a relatively inefficient linear-actuator screw drive, with interference, rather than square or lead-screw threads designed to minimize friction and "thread-

jumping" that resulted in failures in reagent delivery. Last, the NE-100 flow-control mechanism included several parts made of materials (Delrin, Silicone) with low resistance to acid solutions that failed after extended use. We heavily modified the pumps to eliminate these components and ultimately achieved acceptable performance, but alternate delivery mechanisms should be considered (*see* Comments and Recommendations section).

Although we did not detect systematic errors across all trials through visual inspection of sign-retaining percent errors (Fig. 5), *t*-test statistical analyses showed a small bias toward underdelivery of both reagents that was slightly greater for the acid reagent. The reagent underdelivery resulted in mean negative values of % relative error for both TAlk (−0.58%, $t_{376,375} = -2.29$; $p = 0.023$) and TCO_2 (−1.01%, $t_{376,375} = -5.40$; $p < 0.001$). The increase of % relative error and standard deviations (SD) for both TAlk and TCO_2 for the trials conducted between July 2016 and March 2017 is evidence of progressive mechanical fatigue in the syringe pumps, leading to loss of accuracy and precision (Table 1; Fig. 5). Accordingly, we have excluded the 2017 data for further analysis, as the mechanical integrity of some of the syringe pumps seemed significantly compromised and, therefore, the results do not provide a reliable evaluation of the manipulation system.

Decoupling of carbonate chemistry parameters: pH and Ω_{Ar}

DOAMES was generally able to deliver statistically significant experimental treatments that successfully decoupled pH and Ω_{Ar} by producing a range of carbonate chemistry conditions with a common, stable Ω_{Ar} within 0.7 units of target, and across a range of pH values (Tables 2–3; Fig. 6). DOAMES effectively decoupled these carbonate chemistry variables even in the experiments conducted in July and August 2016 (Fig. 6g–j), when syringe pumps' developing mechanical fatigue was already decreasing accuracy and precision of the manipulations (Table 1). Despite the overall success in decoupling of carbonate chemistry parameters, there were, however, several instances of high pH experimental treatment overlapping with the medium pH treatment (Fig. 6b,f,j), resulting in treatments not being statistically different from each other. Overlapping in treatments result from the disproportionate effect of small, opposite signs % relative errors of TAlk and TCO_2 on pH in the least manipulated chemistries (i.e., lowest absolute values of TAlk and TCO_2).

Although the observed variability in Ω_{Ar} and pH in our trials is greater than usually found in published laboratory studies conducted through precise CO_2 gas injections (i.e., pH up to 0.03 units in SD and up to 0.4 SD units for Ω_{Ar}; Talmage and Gobler 2010; Hettinger et al. 2012; Barros et al. 2013), our results are still within the variability of published batch-culture studies aimed at decoupling carbonate chemistry parameters (Gazeau et al. 2011; Thomsen et al. 2015*a*; Waldbusser et al. 2015*a*, *b*, 2016*b*). DOAMES is, therefore, performing within the range of current community standards for the types of manipulations we are conducting.

Dynamic source seawater input and variable targets test

Under moderately variable source seawater conditions (Fig. 7), DOAMES simultaneously produced stable, dynamic, and offset experimental treatments by using each of the three controller channels for a given manipulation (Fig. 8).

Although we achieved a moderately dynamic source seawater (Fig. 7), the continuous seawater streamflow at HMSC laboratories originates from HMSC facility-wide reservoir tanks that do not fill continuously. Rather, seawater is pumped twice a day during high tide from Yaquina Bay, Oregon, and stored in reservoir tanks for

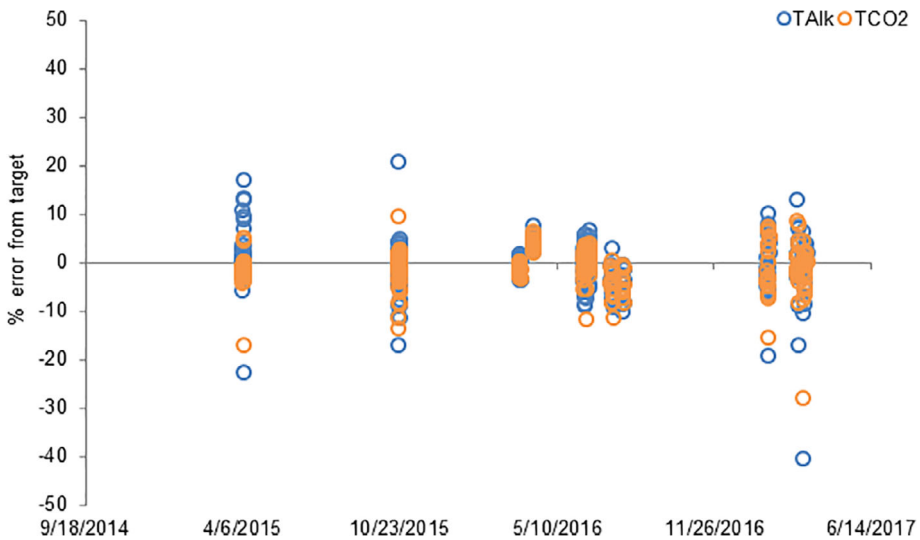

Fig. 5. Timeline of multiple time-series of % signed relative error from targets from discrete samples of TAlk (blue) and TCO_2 (orange). Slight underdelivery of both chemical reagents was detected. Increased variability in 2017 trials was the result of mechanical fatigue of the reagent pumps (*see* Assessment and Discussion sections).

Table 3. One-way ANOVA of Ω_{Ar} and pH_t decoupling experiments.

Date	Source of pH_t Variance	Degrees of freedom	Sums of squares	*F* value	*p* value
October 2015	Treatment	2	1.080	27.54	<0.0001
	Error	61	1.196		
March 2016	Treatment	2	0.606	118.10	<0.0001
	Error	51	0.131		
April 2016	Treatment	2	0.115	11.96	0.0029
	Error	9	0.043		
July 2016	Treatment	2	0.159	12.07	0.0005
	Error	18	0.119		
August 2016	Treatment	2	0.113	6.23	0.0116
	Error	14	0.126		

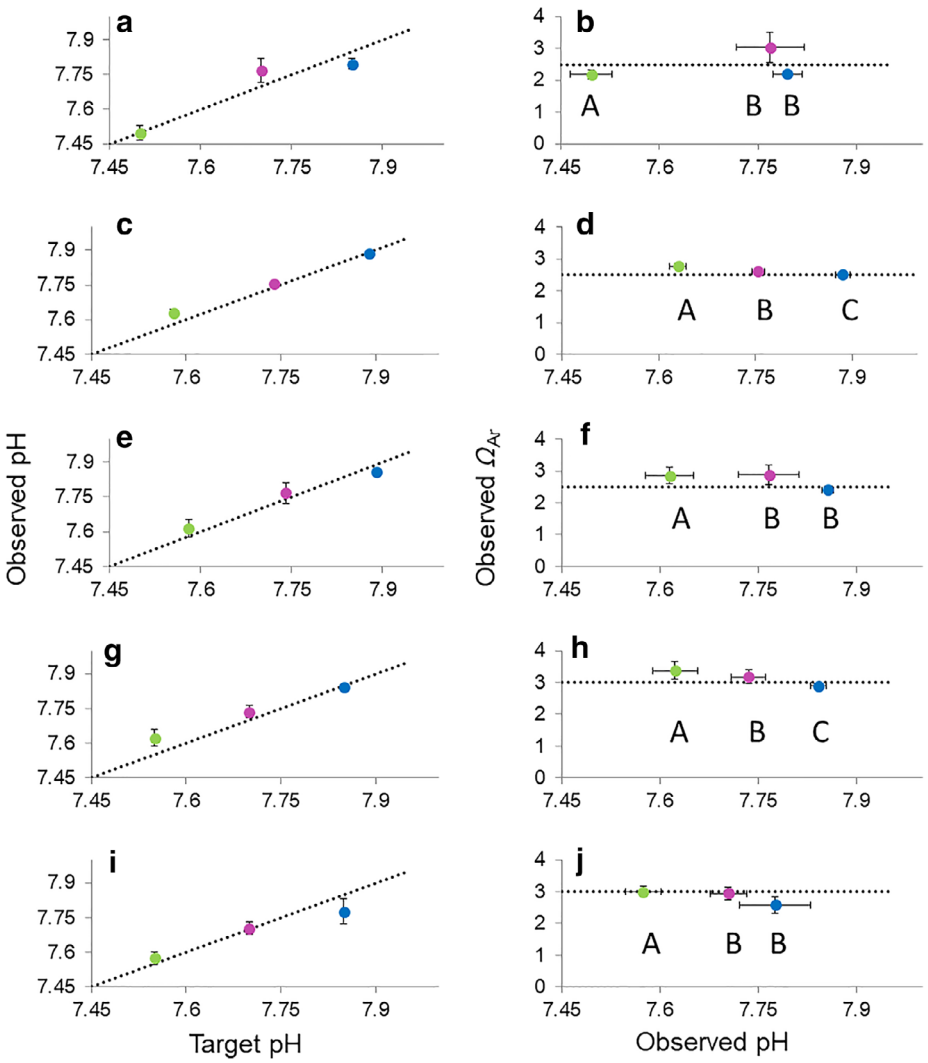

Fig. 6. Examples of multiple manipulation experiments targeting constant Ω_{Ar} and varying pH levels. Each color corresponds to one manipulation channel. Error bars are standard errors. Dotted line represents complete agreement between target and observations on $pH_{observed}$ vs. pH_{target} plots (i.e., left panels) and target Ω_{Ar} in observed Ω_{Ar} vs. observed pH plots (i.e., right panels). (**a**, **b**) Experiment conducted in October 2015; (**c**, **d**) experiment conducted in March 2016; (**e**, **f**) experiment conducted in April 2016; (**g**, **h**) experiment conducted in July 2016; and (**i**, **j**) experiment conducted in August 2016. Capital letters correspond to Tukey multiple comparisons on arcsine square root transformed proportions, $p < 0.1$.

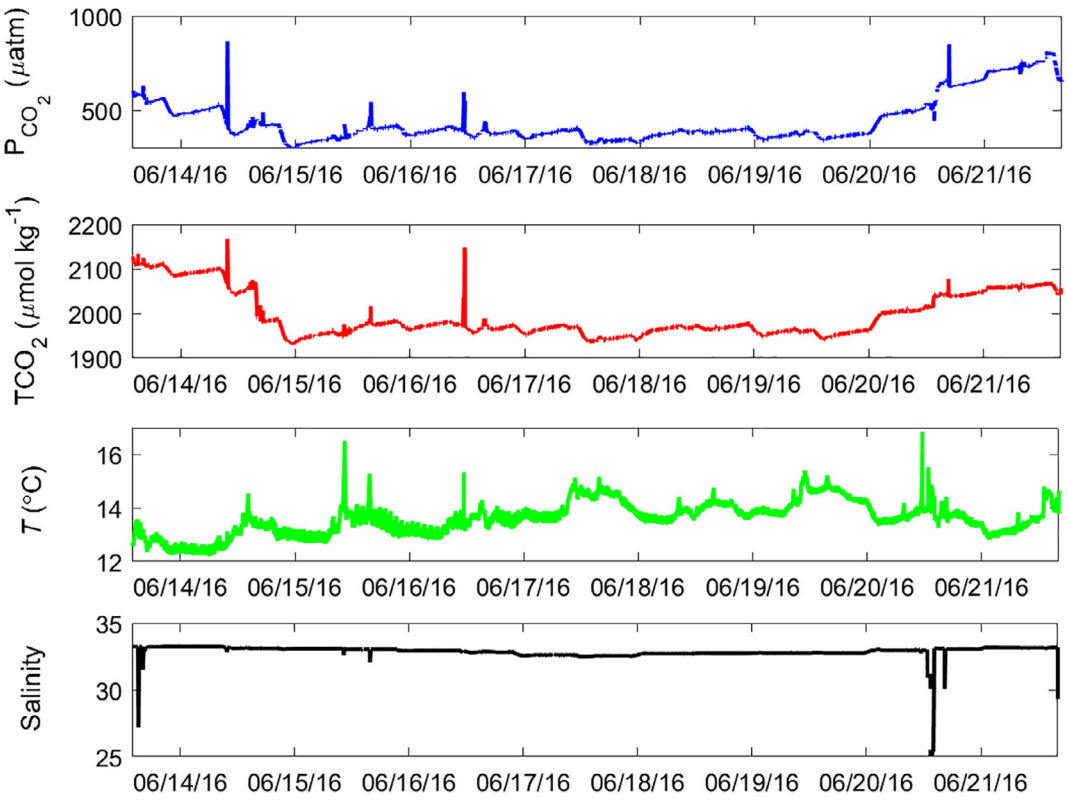

Fig. 7. Time-series of source seawater conditions during the experiment with stable, dynamic, and offset simultaneous target manipulations. Note that abrupt changes in parameters are linked to the refilling of reservoir tanks (*see* Discussion section). Brief drops in salinity values are the result of transient dilution of seawater after the switch of seawater lines and were not captured in the TCO_2 time-series, because TCO_2 measurements were only performed one to four times per hour.

further distribution through HMSC laboratories, effectively dampening the high-frequency natural variability expected from a tidally influenced estuary (Barton et al. 2012; Hales et al. 2017).

The combined precision and accuracy across the three manipulation channels is better than DOAMES overall values, with overall better performance in obtaining TCO_2 targets relative to TAlk (Table 1). We then assessed each manipulation channel potential performance and potential for systematic errors by evaluating their mean signed-retaining error. For the stable treatment, both TCO_2 and TAlk manipulations achieved great accuracy and performed similarly regarding precision ($-0.2\% \pm 2.7\%$ for TCO_2 compared to $-0.1\% \pm 2.7\%$ for TAlk). The idealized TCO_2 dynamic treatment performed slightly worse in terms of accuracy for both TCO_2 and TAlk but better for TCO_2 precision ($1.1\% \pm 1.6\%$ for TCO_2; $-0.6\% \pm 3.8\%$ for TAlk) when compared to the stable target manipulation. Finally, the best performing manipulation channel was the dynamic offset ($-0.0\% \pm 1\%$ for TCO_2 compared to $1.6\% \pm 1.4\%$ for TAlk), which is to be expected considering that it is the least "manipulated" system and, therefore, requires the lowest reagent additions. These results suggest that DOAMES is indeed capable of responding to dynamic source seawater inputs and to simultaneously produce stable and dynamic treatments with TCO_2 and TAlk targets that range across 2050 to 2950 μmol kg^{-1}.

Larval exposure experiment

Bivalve embryos developed normally on DOAMES-manipulated water that was stripped of ~ 80% of the TCO_2 and TAlk (Fig. 9; Table 4) and then returned to conditions that mimicked control seawater. Manipulated conditions were, on average, approximately 0.3% lower for TCO_2, close to analytical uncertainty, and 1.9% greater for TAlk with respect to the static control (Table 4). These unequal deviations from TAlk and TCO_2 targets resulted in slightly elevated mean Ω_{Ar} and pH values in the flow-through manipulated water with respect to the static control (Table 4). These deviations, however, are less than 0.5 units Ω_{Ar} and 0.06 for pH, within the experimental conditions variability reported on other carbonate chemistry parameter decoupling studies (Gazeau et al. 2011; Thomsen et al. 2015*a*, *b*; Waldbusser et al. 2015*b*, 2016*b*).

Bivalve larval development at 48 h postfertilization was not statistically different in control-simulating manipulated water treatment compared to untreated control water (Fig. 9). The mean percentage of normally developed larvae was $90.9\% \pm 1.5\%$ for the static control, $88.1\% \pm 5.6\%$ for the flow-through control, $86.0\% \pm 3.3\%$ for the manipulated flow-through treatment, $81.6\% \pm 2.6\%$ for the manipulated static, and $0.2\% \pm 0.4\%$ for the unmanipulated static. These developmental responses agree with published results on early Pacific oyster larvae development

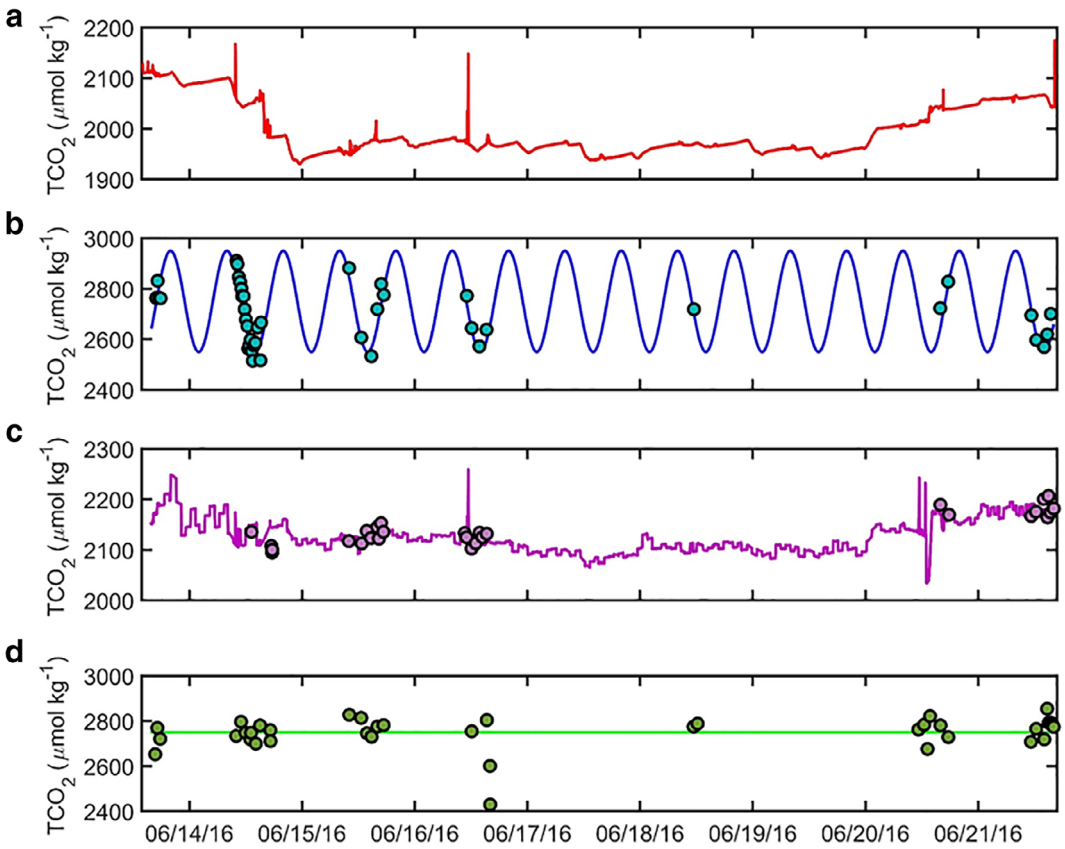

Fig. 8. Stable, dynamic, and offset TCO_2 manipulations with moderately dynamic source seawater input. (**a**) In red, source seawater TCO_2 time-series during the manipulation experiment. (**b**) In solid blue, idealized sinusoid TCO_2 target for dynamic manipulation treatment. Blue/green dots are discrete samples from this dynamic treatment. (**c**) In solid pink, offset TCO_2 target based on ΔPCO_2 projections for 2100 under RCP6.0. Pink dots are discrete samples from this offset treatment. (**d**) In solid green, TCO_2 target for stable manipulation treatment. Green dots represent discrete samples from this stable treatment.

that identified a favorable threshold of $\Omega_{Ar} > \sim 2.3$ that corresponded with more that 80% normally developed larvae and a sensitivity threshold of $\Omega_{Ar} < 1.4$ that was associated with significant proportions of abnormal larvae present (Waldbusser et al. 2015*a*). It is important to note that one of the five replicates of the manipulated, static treatment resulted in near-zero normal development. Upon further analysis of the carbonate chemistry, we hypothesize that the BOD bottle was probably filled with a combination of manipulated and transient unmanipulated water, as the TAlk and TCO_2 values were consistent with partially manipulated water. We speculate that this replicate bottle was filled before the manipulation system had stabilized and, as a result, was excluded from further analysis.

We found a highly significant effect of treatment on development to day 2 postfertilization (Table 5; $F_{4,19} = 536.7$, $p < 0.0001$), mostly driven by the detrimental effects of the unmanipulated treatment. Indeed, upon further exploration of the post hoc multiple comparisons, we found no significant differences among controls (both static and flow-through) and the flow-through, manipulated water (Fig. 9).

These results suggest that DOAMES allows for the adequate development of embryos in a flow-through environment and that there are no inherent negative effects of manipulated water to mimic control seawater conditions on larvae development. We, therefore, conclude that this is a successful proof-

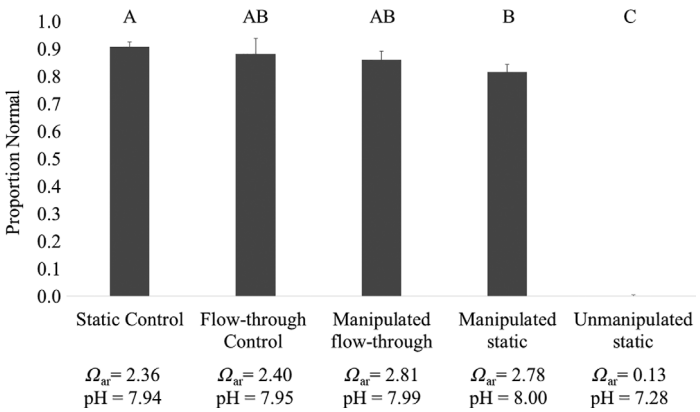

Fig. 9. Proportion of normally developed Pacific oyster (*C. gigas*) at 48 h postfertilization. Error bars are SD of replicate culture chambers per treatment ($n = 5$, except for manipulated static $n = 4$). Carbonate chemistry parameters correspond to the carbonate chemistry conditions for each treatment shown in Table 4. Letters correspond to Tukey multiple comparisons on arcsine square root transformed proportions, $p < 0.1$.

Table 4. Experimental conditions in 2015 Pacific oyster larval experiment.

Treatment	Temperature (°C)	Salinity	TAlk (μmol kg^{-1})	TCO_2 (μmol kg^{-1})	PCO_2 (μatm)	pHt	Ω_{Ca}	Ω_{Ar}
Static control	25.0	29.0	2125	1934	515	7.94	3.54	2.36
Flow-through control	25.0	29.0	2121	1926	502	7.95	3.60	2.40
Flow-through manipulated	25.0	30.8	2166	1928	485	7.99	4.22	2.81
Manipulated static	25.0	30.9	2185	1948	436	8.00	4.17	2.78
Unmanipulated static	25.0	29.9	460	452	562	7.28	0.19	0.13

of-concept of the suitability of our novel manipulation system for experimental work on marine organisms.

Discussion

DOAMES proof-of-concept results demonstrate its capability to decouple Ω_{Ar} and pH in a flow-through setting, a key tool to determine chronic organismal and population-level sensitivities to past, current, and future carbonate chemistry scenarios and, ultimately, provide adequate forecasts of the future fate of taxa vulnerable to OA. Indeed, DOAMES-manipulated water supported normal embryo development during the most vulnerable stage of bivalve larvae. As the organismal exposure experiment discussed here, we have since utilized DOAMES to successfully raise fertilized embryos to 48 h old larvae at seven times higher organismal densities (200 embryos mL^{-1}) and 13 times higher flow rates (~ 14 mL min^{-1}; Langdon et al. unpubl.). DOAMES, therefore, can support experimental work that requires elevated densities of organisms due to either expected high initial mortality (White et al. 2013) or the need for abundant biomass for specific analysis (e.g., transcriptomics [De Wit et al. 2018] and lipid extraction [Waldbusser et al. 2016*b*; Brunner et al. 2016]). DOAMES flow-through capabilities support experimental designs that need higher flows to optimize organismal development (e.g., Howes et al. 2014) or when deviations from target carbonate chemistry conditions as a result of metabolic processes need to be minimized (e.g., Gradoville et al. 2014). Additionally, DOAMES flow-through configuration allows for long experimental exposures (e.g., Ginger et al. 2013) and multigenerational experiments of organisms (e.g., Parker et al. 2015; Griffith and Gobler 2017), providing an empirical framework to explore potential differential carry-over effects (e.g., Hettinger et al. 2012, 2013) of exposure to different carbonate chemistry parameters.

Table 5. One-way ANOVA of Pacific oyster (*C. gigas*) early larval development in response to carbonate chemistry treatment.

Source of variance	Degrees of freedom	Sums of squares	*F* value	*p* value
Treatment	4	5.625	536.7	<0.0001
Error	19	0.050		

DOAMES supports experimental treatments with dynamic TCO_2 (or TAlk) targets, simulating carbonate chemistry variability naturally found in coastal systems to assess its effects on organismal physiology. Although determining organismal responses to naturally variable carbonate chemistry conditions is an identified research priority within the OA community (Boyd et al. 2016; Wahl et al. 2016), variable carbonate chemistry conditions are technically difficult to recreate in laboratory settings, and the development of experimental systems capable of dynamic treatments is recent (Frieder et al. 2014; Burrell et al. 2016; Clark and Gobler 2016; Eriander et al. 2016; Kapsenberg et al. 2017; Onitsuka et al. 2018). DOAMES dynamic target mode allows for the exploration of the effects of high- and low-frequency carbonate chemistry variable conditions and comparison of physiological responses to those of stable treatments, thereby providing empirical evidence to help reconcile observed divergent responses across multiple taxa and life-stages.

Carbonate chemistry variable treatments have been shown to mitigate, exacerbate, or elicit the same physiological response when compared to stable OA treatments in species such as microalgae and macroalgae (Cornwall et al. 2013; Li et al. 2016), bivalve larvae (Frieder et al. 2014; Clark and Gobler 2016; Eriander et al. 2016), adult bivalves (Keppel et al. 2015), recruits and adult corals (Dufault et al. 2012), and fish (Jarrold 2017). DOAMES' flexibility to incorporate complex dynamic TAlk and TCO_2 target regimes also supports the design of experiments that can test the relative impact of transient extremes on organisms, previously identified as important drivers of physiological responses to temperature (Helmuth et al. 2010). Ultimately, DOAMES' ability to create complex but controlled dynamic exposures to OA enables the testing and validation of stress indexes designed to capture physiological stress due to variable natural conditions (e.g., Gimenez et al. 2018).

Additionally, DOAMES is capable of mimicking future environmental conditions on variable coastal environments by applying system-specific offsets based on CO_2 emission scenarios to naturally variable carbonate chemistry conditions. In this work, we tested the ΔPCO_2 approach to simulate future OA conditions (Feely et al. 2010; Hales et al. 2017; Pacella et al. 2018), assuming constant disequilibrium between atmospheric CO_2 and seawater PCO_2. We believe, however, that DOAMES is capable of projecting future conditions based on the ΔTCO_2 method (Pacella et al. 2018, and references therein) that assumes constant disequelibrium

between the measured TCO_2 and the computed TCO_2 if the observed system was in equilibrium, likely a more appropriate method for coastal environments, where metabolic processes significantly affect the carbonate chemistry and their buffering capacity. Experimental designs that involve carbonate parameter decoupling or variable environmental conditions are technically complex and require high precision in the chemical manipulations and therefore are particularly challenging in longer term experiments.

DOAMES' high degree of automation requires minimal user-input to initialize an experiment, and its feed-forward control logic reduces hysteresis and provides stability to the manipulated treatments, even in highly complex experimental designs as the dynamic and offset targets discussed above. Some of the published flow-through experimental systems designed for OA experiments rely on sufficently long gas equilibration times to ensure experimental treatment stability (e.g., Fangue et al. 2010; Eriander et al. 2016). Conversely, the experimental systems that do rely in some control logic almost invariably do so by using feed-back control (McGraw et al. 2010; Burrell et al. 2016; Sordo et al. 2016; Wahl et al. 2016).

For reasonably constrained systems, feed-forward control is a viable option that provides increased stability and, presumably, reduced hysteresis when compared to feed-back–controlled systems (Hovd and Bitmead 2009). Constrained systems are those for which the most important controlling variables are known and measurable and their effect on the output can be fully predicted. The carbonate system, governed by well-known thermodynamic relationships, can be therefore considered a constrained system and, therefore, suitable for feed-forward control. We acknowledge that the ideal experimental system would incorporate an adaptive feed-forward or a combination of feed-forward and feed-back controllers, although this approach is often unfeasible due to logistical and financial constraints. For DOAMES, a dual feed-forward and feed-back approach would require an additional PCO_2/TCO_2 analyzer downstream from the manipulation channels that would continuously monitor both parameters for each channel and, more importantly, a complex logic to adjust future manipulation targets balancing both the input from the source seawater carbonate chemistry signature and the measured experimental conditions.

Comments and recommendations

DOAMES modular flexibility allows for multiple manipulation channels and different experimental treatment configurations, including simultaneous coupling or decoupling of carbonate variables, and stable, dynamic, and offset carbonate chemistry targets. The current proof-of-concept system described in this work includes three simultaneous manipulation channels, but we can foresee the addition of more with minimal software changes. Thus, DOAMES affords experimentalists a high degree of customization to tailor to their specific research needs and can be replicated by future users within a few months, considering time required for installation and validation. We provide some suggestions to facilitate its adaptation.

First, the constraint of processes inherent to the experimental design that can lead to deviations from targets is key in feed-forward controlled systems like DOAMES. We suggest, therefore, that future DOAMES users should consider exploring alternative reagent delivery systems, as DOAMES' current reagent injection design is responsible for most of the deviations from targeted manipulation values and for the small but significant systematic underdelivery of base and acid reagents. Within the injection system, the weakest component has been identified: the syringe pumps.

Syringe pumps are very affordable, easy to program and interface with the manipulation controller software, and they can provide precise volume delivery across an extended range of flow rates. These attributes originally made syringe pumps an obvious choice for DOAMES; however, alternative reagent delivery systems that minimize the need for switching valves and limit mechanical fatigue that can lead to manipulation errors will reduce the frequency of reagent delivery failures and, thus, increase DOAMES' robustness. We suggest, therefore, alternative options as programmable, high-precision peristaltic, or valve-less metering pumps. Although significantly more expensive, these pumps will eliminate the need of having dual syringe pumps per reagent and channel, as they can deliver volume continuously and therefore, also mitigate the need for switching valves. Regardless of the reagent delivery system selected, we suggest collection of a minimum of daily discrete carbonate chemistry samples for treatment validation.

Second, selecting the right combination of reagent pumps depends on the desired carbonate chemistry targets and the required total experimental treatment seawater flow rate (i.e., flow rate to each replicate culture chambers multiplied by total number of replicates). As a first approximation, however, reagent flow rates are typically less than 10% of the total experimental treatment seawater flow rate, even if the source seawater has been stripped of TCO_2 and TAlk. We suggest, therefore, that first users identify the total flow required and then select the appropriate combination of reagent pumps to suit their needs.

Finally, we suggest the use of intermediate holding seawater tanks for manipulated water when designing low flow, high residence-time experiments. Although the use of pumps that can continuously deliver reagents will significantly lower the occurrence of manipulation errors associated with reagent delivery failures, transient breaks in carbonate chemistry manipulations can still occur. Instances of delivery of undermanipulated or unmanipulated water can have an outsized effect in low flow, high residence time experimental designs; thus, an intermediate holding seawater tank can buffer high-frequency variability resulting from brief manipulation errors and produce experimental treatments with very stable carbonate chemistry. We recommend optimizing the volume of these intermediate holding tanks to ensure adequate flushing rates that limit bacterial growth that could result in decreased overall water quality.

References

Archer, D. E., T. Takahashi, S. Sutherland, J. Goddard, D. Chipman, K. Rodgers, and H. Ogura. 1996. Daily, seasonal and interannual variability of sea-surface carbon and nutrient concentration in the equatorial Pacific Ocean. Deep Sea Res. Part II Top. Stud. Oceanogr. **43**: 779–808. doi:10.1016/0967-0645(96)00017-3

Bach, L. T., L. C. M. Mackinder, K. G. Schulz, G. Wheeler, D. C. Schroeder, C. Brownlee, and U. Riebesell. 2013. Dissecting the impact of CO_2 and pH on the mechanisms of photosynthesis and calcification in the coccolithophore Emiliania huxleyi. New Phytol. **199**: 121–134. doi:10.1111/nph.12225

Bandstra, L., B. Hales, and T. Takahashi. 2006. High-frequency measurements of total CO_2: Method development and first oceanographic observations. Mar. Chem. **100**: 24–38. doi:10.1016/j.marchem.2005.10.009

Barros, P., P. Sobral, P. Range, L. Chícharo, and D. Matias. 2013. Effects of sea-water acidification on fertilization and larval development of the oyster *Crassostrea gigas*. J. Exp. Mar. Biol. Ecol. **440**: 200–206. doi:10.1016/j.jembe.2012.12.014

Barton, A., B. Hales, G. G. Waldbusser, C. Langdon, and R. A. Feely. 2012. The Pacific oyster, *Crassostrea gigas*, shows negative correlation to naturally elevated carbon dioxide levels: Implications for near-term ocean acidification effects. Limnol. Oceanogr. **57**: 698–710. doi:10.4319/lo.2012.57.3.0698

Bates, N. R., T. Takahashi, D. W. Chipman, and A. H. Knap. 1998. Variability of pCO_2 on diel to seasonal timescales in the Sargasso Sea near Bermuda. J. Geophys. Res. Oceans **103**: 15567–15,585. doi:10.1029/98JC00247

Bates, N. R., M. H. P. Best, K. Neely, R. Garley, A. G. Dickson, and R. J. Johnson. 2012. Detecting anthropogenic carbon dioxide uptake and ocean acidification in the North Atlantic Ocean. Biogeosci. Discuss. **9**: 989–1019. doi:10.5194/bgd-9-989-2012

Bates, N., Y. Astor, M. Church, K. Currie, J. Dore, M. Gonaález-Dávila, L. Lorenzoni, F. Muller-Karger, J. Olafsson, and M. Santa-Casiano. 2014. A time-series view of changing ocean chemistry due to ocean uptake of anthropogenic CO_2 and ocean acidification. Oceanography **27**: 126–141. doi:10.5670/oceanog.2014.16

Boyd, P. W., C. E. Cornwall, A. Davison, S. C. Doney, M. Fourquez, C. L. Hurd, I. D. Lima, and A. McMinn. 2016. Biological responses to environmental heterogeneity under future ocean conditions. Glob. Chang. Biol. **22**: 2633–2650. doi:10.1111/gcb.13287

Brunner, E., F. Prahl, B. Hales, and G. Waldbusser. 2016. A longitudinal study of Pacific oyster (*Crassostrea gigas*) larval development: isotope shifts during early shell formation reveal sub-lethal energetic stress. Mar. Ecol. Prog. Ser. **555**: 109–123. doi:10.3354/meps11828

Burrell, R. B., A. G. Keppel, V. M. Clark, and D. L. Breitburg. 2016. An automated monitoring and control system for flow-through co-cycling hypoxia and pH experiments: Automated co-cycling DO and pH system. Limnol. Oceanogr. Methods **14**: 168–185. doi:10.1002/lom3.10077

Cai, W.-J., and others. 2011. Acidification of subsurface coastal waters enhanced by eutrophication. Nat. Geosci. **4**: 766–770. doi:10.1038/ngeo1297

Caldeira, K., and M. E. Wickett. 2003. Anthropogenic carbon and ocean pH. Nature **425**: 365. doi:10.1038/425365a

Cigliano, M., M. C. Gambi, R. Rodolfo-Metalpa, F. P. Patti, and J. M. Hall-Spencer. 2010. Effects of ocean acidification on invertebrate settlement at volcanic CO_2 vents. Mar. Biol. **157**: 2489–2502. doi:10.1007/s00227-010-1513-6

Clark, H., and C. Gobler. 2016. Diurnal fluctuations in CO_2 and dissolved oxygen concentrations do not provide a refuge from hypoxia and acidification for early-life-stage bivalves. Mar. Ecol. Prog. Ser. **558**: 1–14. doi:10.3354/meps11852

Comeau, S., and others. 2017. Coral calcifying fluid pH is modulated by seawater carbonate chemistry not solely seawater pH. Proc. R. Soc. B Biol. Sci. **284**: 20161669. doi:10.1098/rspb.2016.1669

Cornwall, C. E., C. D. Hepburn, C. M. McGraw, K. I. Currie, C. A. Pilditch, K. A. Hunter, P. W. Boyd, and C. L. Hurd. 2013. Diurnal fluctuations in seawater pH influence the response of a calcifying macroalga to ocean acidification. Proc. R. Soc. B Biol. Sci. **280**: 20132201. doi:10.1098/rspb.2013.2201

Cornwall, C. E., and C. L. Hurd. 2015. Experimental design in ocean acidification research: Problems and solutions. ICES J. Mar. Sci. J. Cons. **73**: fsv118–fsv581. doi:10.1093/icesjms/fsv118

Crame, J. A. 2000. Evolution of taxonomic diversity gradients in the marine realm: Evidence from the composition of recent bivalve faunas. Paleobiology **26**: 188–214. doi:10.1666/0094-8373(2000)026<0188:EOTDGI>2.0.CO;2

Cyronak, T., K. G. Schulz, and P. L. Jokiel. 2016. The omega myth: What really drives lower calcification rates in an acidifying ocean. ICES J. Mar. Sci. J. Cons. **73**: 558–562. doi:10.1093/icesjms/fsv075

DeGrandpre, M. D., R. Wanninkhof, W. R. McGillis, and P. G. Strutton. 2004. A Lagrangian study of surface pCO_2 dynamics in the eastern equatorial Pacific Ocean. J. Geophys. Res. Oceans **109**: C08S07. doi:10.1029/2003JC002089

De Wit, P., E. Durland, A. Ventura, and C. J. Langdon. 2018. Gene expression correlated with delay in shell formation in larval Pacific oysters (*Crassostrea gigas*) exposed to experimental ocean acidification provides insights into shell formation mechanisms. BMC Genomics **19**. doi:10.1186/s12864-018-4519-y

Dickson, A. G. 1990. Thermodynamics of the dissociation of boric acid in synthetic seawater from 273.15 to 318.15 K. Deep Sea Research **37**: 755–766. doi:10.1016/0198-0149(90)90004-F

Doney, S. C., V. J. Fabry, R. A. Feely, and J. A. Kleypas. 2009. Ocean acidification: The other CO_2 problem. Annu. Rev. Mar. Sci. **1**: 169–192. doi:10.1146/annurev.marine.010908.163834

Dore, J. E., R. Lukas, D. W. Sadler, M. J. Church, and D. M. Karl. 2009. Physical and biogeochemical modulation of ocean acidification in the central North Pacific. Proc. Natl. Acad. Sci. USA **106**: 12235–12240. doi:10.1073/pnas.0906044106

Dufault, A. M., V. R. Cumbo, T.-Y. Fan, and P. J. Edmunds. 2012. Effects of diurnally oscillating pCO_2 on the calcification and survival of coral recruits. Proc. R. Soc. B Biol. Sci. **279**: 2951–2958. doi:10.1098/rspb.2011.2545

Eriander, L., A.-L. Wrange, and J. N. Havenhand. 2016. Simulated diurnal pH fluctuations radically increase variance in—But not the mean of—Growth in the barnacle *Balanus improvisus*. ICES J. Mar. Sci. J. Cons. **73**: 596–603. doi:10.1093/icesjms/fsv214

Evans, W., J. T. Mathis, J. Ramsay, and J. Hetrick. 2015. On the frontline: Tracking ocean acidification in an Alaskan shellfish hatchery. PLoS One **10**: e0130384. doi:10.1371/journal.pone.0130384

Fangue, N. A., M. J. O'Donnell, M. A. Sewell, P. G. Matson, A. C. MacPherson, and G. E. Hofmann. 2010. A laboratory-based, experimental system for the study of ocean acidification effects on marine invertebrate larvae. Limnol. Oceanogr. Methods **8**: 441–452. doi:10.4319/lom.2010.8.441

Fassbender, A. J., C. L. Sabine, and K. M. Feifel. 2016. Consideration of coastal carbonate chemistry in understanding biological calcification: Coastal zone calcification. Geophys. Res. Lett. **43**: 4467–4476. doi:10.1002/2016GL068860

Feely, R. A. 2004. Impact of anthropogenic CO_2 on the $CaCO_3$ system in the oceans. Science **305**: 362–366. doi:10.1126/science.1097329

Feely, R. A., S. R. Alin, J. Newton, C. L. Sabine, M. Warner, A. Devol, C. Krembs, and C. Maloy. 2010. The combined effects of ocean acidification, mixing, and respiration on pH and carbonate saturation in an urbanized estuary. Estuar. Coast. Shelf Sci. **88**: 442–449. doi:10.1016/j.ecss.2010.05.004

Frieder, C. A., J. P. Gonzalez, E. E. Bockmon, M. O. Navarro, and L. A. Levin. 2014. Can variable pH and low oxygen moderate ocean acidification outcomes for mussel larvae? Glob. Chang. Biol. **20**: 754–764. doi:10.1111/gcb.12485

Gattuso, J.-P., K. Gao, K. Lee, B. Rost, and K. G. Schulz. 2010. Approaches and tools to manipulate the carbonate chemistry, p. 13. *In* U. Riebesell, V. J. Fabry, L. Hansson, and J.-P. Gattuso [eds.], Guide for Best practices in ocean acidification research and data reporting. Publications Office of the European Union. doi:10.2777/66906

Gazeau, F., J.-P. Gattuso, M. Greaves, H. Elderfield, J. Peene, C. H. R. Heip, and J. J. Middelburg. 2011. Effect of carbonate chemistry alteration on the early embryonic development of the Pacific oyster (*Crassostrea gigas*). PLoS One **6**: e23010. doi:10.1371/journal.pone.0023010

Gimenez, I., G. G. Waldbusser, and B. Hales. 2018. Ocean acidification stress index for shellfish (OASIS): Linking Pacific oyster larval survival and exposure to variable carbonate chemistry regimes. Elem Sci Anth **6**: 51. doi:10.1525/elementa.306

Ginger, K. W. K., C. B. S. Vera, D. R, C. K. S. Dennis, L. J. Adela, Z. Yu, and V. Thiyagarajan. 2013. Larval and post-larval stages of Pacific oyster (*Crassostrea gigas*) are resistant to elevated CO_2. PLoS One **8**: e64147. doi:10.1371/journal.pone.0064147

Gradoville, M. R., A. E. White, and R. M. Letelier. 2014. Physiological response of Crocosphaera watsonii to enhanced and fluctuating carbon dioxide conditions. PLoS One **9**: e110660. doi:10.1371/journal.pone.0110660

Gray, M., C. Langdon, G. Waldbusser, B. Hales, and S. Kramer. 2017. Mechanistic understanding of ocean acidification impacts on larval feeding physiology and energy budgets of the mussel *Mytilus californianus*. Mar. Ecol. Prog. Ser. **563**: 81–94. doi:10.3354/meps11977

Griffith, A. W., and C. J. Gobler. 2017. Transgenerational exposure of North Atlantic bivalves to ocean acidification renders offspring more vulnerable to low pH and additional stressors. Sci. Rep. **7**: 11394. doi:10.1038/s41598-017-11,442-3

Hales, B., D. Chipman, and T. Takahashi. 2004. High-frequency measurement of partial pressure and total concentration of carbon dioxide in seawater using microporous hydrophobic membrane contactors. Limnology and Oceanography: Methods **2**: 356–364. doi:10.4319/lom.2004.2.356

Hales, B., A. Suhrbier, G. G. Waldbusser, R. A. Feely, and J. A. Newton. 2017. The carbonate chemistry of the "fattening line," Willapa Bay, 2011–2014. Estuar. Coasts **40**: 173–186. doi:10.1007/s12237-016-0136-7

Helmuth, B., B. R. Broitman, L. Yamane, S. E. Gilman, K. Mach, K. A. S. Mislan, and M. W. Denny. 2010. Organismal climatology: Analyzing environmental variability at scales relevant to physiological stress. J. Exp. Biol. **213**: 995–1003. doi:10.1242/jeb.038463

Hettinger, A., E. Sanford, T. M. Hill, E. A. Lenz, A. D. Russell, and B. Gaylord. 2013. Larval carry-over effects from ocean acidification persist in the natural environment. Glob. Change Biol. **19**: 3317–3326. doi:10.1111/gcb.12307

Hettinger, A., E. Sanford, T. M. Hill, A. D. Russell, K. N. S. Sato, J. Hoey, M. Forsch, H. N. Page, and B. Gaylord. 2012. Persistent carry-over effects of planktonic exposure to ocean acidification in the Olympia oyster. Ecology **93**: 2758–2768. doi:10.1890/12-0567.1

His, E., M. N. L. Seaman, and R. Beiras. 1997. A simplification the bivalve embryogenesis and larval development bioassay method for water quality assessment. Water Res. **31**: 351–355. doi:10.1016/S0043-1354(96)00244-8

Honisch, B., and others. 2012. The geological record of ocean acidification. Science **335**: 1058–1063. doi:10.1126/science.1208277

Hovd, M., and R. R. Bitmead. 2009. Feedforward for stabilization. IFAC Proc. Vol. **42**: 602–606. doi:10.3182/20090712-4-TR-2008.00097

Howes, E. L., and others. 2014. Sink and swim: A status review of thecosome pteropod culture techniques. J. Plankton Res. **36**: 299–315. doi:10.1093/plankt/fbu002

Jarrold, M. 2017. Diel CO_2 cycles reduce severity of behavioural abnormalities in coral reef fish under ocean acidification. Sci. Rep. **7**: 10153. doi:10.4225/28/5923bfed71f8d

Jokiel, P. L. 2013. Coral reef calcification: Carbonate, bicarbonate and proton flux under conditions of increasing ocean acidification. Proc. R. Soc. B Biol. Sci. **280**: 20130031. doi:10.1098/rspb.2013.0031

Jury, C. P., R. F. Whitehead, and A. M. Szmant. 2010. Effects of variations in carbonate chemistry on the calcification rates of *Madracis auretenra* (= *Madracis mirabilis sensu* Wells, 1973): Bicarbonate concentrations best predict calcification rates. Glob. Chang. Biol. **16**: 1632–1644. doi:10.1111/j.1365-2486.2009.02057.x

Kapsenberg, L., E. E. Bockmon, P. J. Bresnahan, K. J. Kroeker, J.-P. Gattuso, and T. R. Martz. 2017. Advancing ocean acidification biology using Durafet® pH electrodes. Front. Mar. Sci. **4**. doi:10.3389/fmars.2017.00321

Keppel, A., D. Breitburg, G. Wikfors, R. Burrell, and V. Clark. 2015. Effects of co-varying diel-cycling hypoxia and pH on disease susceptibility in the eastern oyster *Crassostrea virginica*. Mar. Ecol. Prog. Ser. **538**: 169–183. doi:10.3354/meps11479

Keul, N., G. Langer, L. J. de Nooijer, and J. Bijma. 2013. Effect of ocean acidification on the benthic foraminifera ammonia sp. is caused by a decrease in carbonate ion concentration. Biogeosciences **10**: 6185–6198. doi:10.5194/bg-10-6185-2013

Kroeker, K. J., R. L. Kordas, R. Crim, I. E. Hendriks, L. Ramajo, G. S. Singh, C. M. Duarte, and J.-P. Gattuso. 2013. Impacts of ocean acidification on marine organisms: Quantifying sensitivities and interaction with warming. Glob. Chang. Biol. **19**: 1884–1896. doi:10.1111/gcb.12179

Kroeker, K. J., R. L. Kordas, R. N. Crim, and G. G. Singh. 2010. Meta-analysis reveals negative yet variable effects of ocean acidification on marine organisms: Biological responses to ocean acidification. Ecol. Lett. **13**: 1419–1434. doi:10.1111/j.1461-0248.2010.01518.x

Kroeker, K. J., F. Micheli, M. C. Gambi, and T. R. Martz. 2011. Divergent ecosystem responses within a benthic marine community to ocean acidification. Proc. Natl. Acad. Sci. USA **108**: 14515–14,520. doi:10.1073/pnas.1107789108

Kump, L. R., T. J. Bralower, and A. Ridgwell. 2009. Ocean acidification in deep time. Oceanography **22**: 94–107. doi:10.5670/oceanog.2009.100

Kwiatkowski, L., and J. C. Orr. 2018. Diverging seasonal extremes for ocean acidification during the twenty-first century. Nat. Clim. Chang. **8**: 141–145. doi:10.1038/s41558-017-0054-0

Landschützer, P., N. Gruber, D. C. E. Bakker, I. Stemmler, and K. D. Six. 2018. Strengthening seasonal marine CO_2 variations due to increasing atmospheric CO_2. Nat. Clim. Chang. **8**: 146–150. doi:10.1038/s41558-017-0057-x

Li, F., Y. Wu, D. A. Hutchins, F. Fu, and K. Gao. 2016. Physiological responses of coastal and oceanic diatoms to diurnal fluctuations in seawater carbonate chemistry under two CO_2 concentrations. Biogeosciences **13**: 6247–6259. doi:10.5194/bg-13-6247-2016

McGraw, C. M., C. E. Cornwall, M. R. Reid, K. I. Currie, C. D. Hepburn, P. Boyd, C. L. Hurd, and K. A. Hunter. 2010. An automated pH-controlled culture system for laboratory-based ocean acidification experiments: Automated pH-controlled culture system. Limnol. Oceanogr. Methods **8**: 686–694. doi:10.4319/lom.2010.8.0686

Millero, F. J. 1995. Thermodynamics of the carbon dioxide system in the oceans. Geochim. Cosmochim. Acta **59**: 661–677. doi:10.1016/0016-7037(94)00354-O

Millero, F. J. 2010. Carbonate constants for estuarine waters. Mar. Freshwater Res. **61**: 139. doi:10.1071/MF09254

Mucci, A. 1983. The solubility of calcite and aragonite in seawater at various salinities, temperatures, and one atmopshere total pressure. Am. J. Sci. **283**: 780–799. doi:10.2475/ajs.283.7.780

Onitsuka, T., H. Takami, D. Muraoka, Y. Matsumoto, A. Nakatsubo, R. Kimura, T. Ono, and Y. Nojiri. 2018. Effects of ocean acidification with pCO_2 diurnal fluctuations on survival and larval shell formation of Ezo abalone, Haliotis discus hannai. Mar. Environ. Res. **134**: 28–36. doi:10.1016/j.marenvres.2017.12.015

Pacella, S. R., C. A. Brown, G. G. Waldbusser, R. G. Labiosa, and B. Hales. 2018. Seagrass habitat metabolism increases short-term extremes and long-term offset of CO_2 under future ocean acidification. Proc. Natl. Acad. Sci. USA **201**: 703445. doi:10.1073/pnas.1703445115

Pachauri, R. K., L. Mayer, and Intergovernmental Panel on Climate Change [eds.]. 2015. Climate change 2014: Synthesis report. Intergovernmental Panel on Climate Change.

Parker, L. M., W. A. O'Connor, D. A. Raftos, H.-O. Pörtner, and P. M. Ross. 2015. Persistence of positive carryover effects in the oyster, *Saccostrea glomerata*, following transgenerational exposure to ocean acidification. PLoS One **10**: e0132276. doi:10.1371/journal.pone.0132276

Rost, B., I. Zondervan, and D. Wolf-Gladrow. 2008. Sensitivity of phytoplankton to future changes in ocean carbonate chemistry: Current knowledge, contradictions and research directions. Mar. Ecol. Prog. Ser. **373**: 227–237. doi:10.3354/meps07776

Schneider, K., and J. Erez. 2006. The effect of carbonate chemistry on calcification and photosynthesis in the hermatypic coral *Acropora eurystoma*. Limnol. Oceanogr. **51**: 1284–1293. doi:10.4319/lo.2006.51.3.1284

Shadwick, E. H., T. W. Trull, B. Tilbrook, A. J. Sutton, E. Schulz, and C. L. Sabine. 2015. Seasonality of biological and physical controls on surface ocean CO_2 from hourly observations at the Southern Ocean time series site south of Australia. Glob. Biogeochem. Cycles **29**: 223–238. doi:10.1002/2014GB004906

Sordo, L., R. Santos, J. Reis, A. Shulika, and J. Silva. 2016. A direct CO_2 control system for ocean acidification experiments: Testing effects on the coralline red algae

Phymatolithon lusitanicum. PeerJ **4**: e2503. doi:10.7717/peerj.2503

Takahashi, T., S. C. Sutherland, D. W. Chipman, J. G. Goddard, C. Ho, T. Newberger, C. Sweeney, and D. R. Munro. 2014. Climatological distributions of pH, pCO_2, total CO_2, alkalinity, and $CaCO_3$ saturation in the global surface ocean, and temporal changes at selected locations. Mar. Chem. **164**: 95–125. doi:10.1016/j.marchem.2014.06.004

Takeshita, Y., and others. 2015. Including high-frequency variability in coastal ocean acidification projections. Biogeosciences **12**: 5853–5870. doi:10.5194/bg-12-5853-2015

Talmage, S. C., and C. J. Gobler. 2010. Effects of past, present, and future ocean carbon dioxide concentrations on the growth and survival of larval shellfish. Proc. Natl. Acad. Sci. USA **107**: 17246–17,251. doi:10.1073/pnas.0913804107

Thomsen, J., K. Haynert, K. M. Wegner, and F. Melzner. 2015a. Impact of seawater carbonate chemistry on the calcification of marine bivalves. Biogeosci. Discuss. **12**: 1543–1571. doi:10.5194/bgd-12-1543-2015

Thomsen, J., K. Haynert, K. M. Wegner, and F. Melzner. 2015b. Impact of seawater carbonate chemistry on the calcification of marine bivalves. Biogeosciences **12**: 4209–4220. doi:10.5194/bg-12-4209-2015

Vance, J. M. 2012. Proof-of-concept: Automated high-frequency measurements of PCO_2 and TCO_2 and real-time monitoring of the saturation state of calcium carbonate. Oregon State University. https://ir.library.oregonstate.edu/concern/graduate_projects/br86b7957

Wahl, M., V. Saderne, and Y. Sawall. 2016. How good are we at assessing the impact of ocean acidification in coastal systems? Limitations, omissions and strengths of commonly used experimental approaches with special emphasis on the neglected role of fluctuations. Mar. Freshw. Res. **67**: 25. doi:10.1071/MF14154

Waldbusser, G. G., E. P. Voigt, H. Bergschneider, M. A. Green, and R. I. E. Newell. 2011. Biocalcification in the eastern oyster (*Crassostrea virginica*) in relation to long-term trends in Chesapeake Bay pH. Estuar. Coasts **34**: 221–231. doi:10.1007/s12237-010-9307-0

Waldbusser, G. G., and J. E. Salisbury. 2014. Ocean acidification in the coastal zone from an Organism's perspective: Multiple system parameters, frequency domains, and habitats. Annu. Rev. Mar. Sci. **6**: 221–247. doi:10.1146/annurev-marine-121,211-172,238

Waldbusser, G. G., and others. 2015a. Saturation-state sensitivity of marine bivalve larvae to ocean acidification. Nat. Clim. Chang. **5**: 273–280. doi:10.1038/nclimate2479

Waldbusser, G. G., and others. 2015b. Ocean acidification has multiple modes of action on bivalve larvae. PLoS One **10**: e0128376. doi:10.1371/journal.pone.0128376

Waldbusser, G. G., B. Hales, and B. A. Haley. 2016a. Calcium carbonate saturation state: On myths and this or that stories. ICES J. Mar. Sci. J. Cons. **73**: 563–568. doi:10.1093/icesjms/fsv174

Waldbusser, G. G., and others. 2016b. Slow shell building, a possible trait for resistance to the effects of acute ocean acidification: Slow shell building. Limnol. Oceanogr. **61**: 1969–1983. doi:10.1002/lno.10348

White, M. M., D. C. McCorkle, L. S. Mullineaux, and A. L. Cohen. 2013. Early Exposure of bay scallops (*Argopecten irradians*) to high CO_2 causes a decrease in larval shell growth. PLoS ONE **8**: e61065. doi:10.1371/journal.pone.0061065

Wittmann, A. C., and H.-O. Pörtner. 2013. Sensitivities of extant animal taxa to ocean acidification. Nat. Clim. Chang. **3**: 995–1001. doi:10.1038/nclimate1982

Zeebe, R. E. 2012. History of seawater carbonate chemistry, atmospheric CO_2, and ocean acidification. Annu. Rev. Earth Planet. Sci. **40**: 141–165. doi:10.1146/annurev-earth-042711-105,521

Acknowledgments

This work was supported by National Science Foundation OCE CRI-OA #1041267 to G.G.W., B.R.H., and C.J.L. I.G. completed this work as partial fulfillment of Ph.D. degree requirements. The authors would like to thank Greg Hutchinson for his invaluable help in designing, implementing, and supporting the flow-through organismal culture setup, as well as his numerous contributions during biological tests. The authors are also grateful to Matthew Gray for imaging and analysis of bivalve larvae and general support during biological tests; Dylan Howell and David Madison for their support during manipulation tests; Dale Hubbard and Joe Jennings for technical support in the design and troubleshooting of the carbonate chemistry manipulation system; Stephanie Smith, Cameron Allen, Stephen Pacella, and Jessamyn Johnson for their support during biological tests; Blaine Schoolfield, Evan Durland, Kimberley Preston, and the Molluscan Broodstock Program for general support at HMSC; and Alan Barton, Sue Cudd, and Mark Wiegardt from Whiskey Creek Hatchery for providing *Crassostrea gigas* broodstock. We are also grateful to two anonymous reviewers for helpful comments that greatly improved the final manuscript.

Conflict of Interest

None declared

Submitted 23 August 2018
Revised 19 March 2019
Accepted 03 April 2019

Associate editor: Mike DeGrandpre